LARGE PLASTIC DEFORMATION AND INITIATION OF FRACTURE AT THE TIP OF A CRACK IN PLANE STRAIN *

Robert M. McMeeking †

December 1976

* The text of this report is taken from the Ph.D. Dissertation submitted by the author at Brown University; the degree is to be awarded in June 1977.

† Formerly Research Assistant in Engineering, Brown University; present affiliation is Division of Applied Mechanics, Stanford University, Stanford, California 94305.

DISCLAIMER

I. FINITE DEFORMATION ANALYSIS OF CRACK TIP OPENING IN ELASTIC-PLASTIC MATERIALS AND IMPLICATIONS FOR FRACTURE INITIATION *

Summary Analyses of the stress and strain fields around smoothly blunting crack tips in both non-hardening and hardening elastic-plastic materials, under contained plane strain yielding and subject to mode I opening loads, have been carried out by a finite element method suitably formulated to admit large geometry changes. The results include the crack tip shape and near-tip deformation field, and the crack tip opening displacement has been related to a parameter of the applied load, the J-integral. The hydrostatic stresses near the crack tip are limited due to the lack of constraint on the blunted tip, limiting achievable stress levels except in a very small region around the crack tip in power law hardening materials. The J-integral is found to be path independent except very close to the crack tip in the region affected by the blunted tip. Models for fracture are discussed in the light of these results including one based on the growth of voids. The rate of void growth near the tip in hardening materials seems to be little different from the rate in non-hardening materials when measured in terms of crack tip opening displacement, which leads to a prediction of higher toughness in hardening materials. It is suggested that improvement of this model would follow from better understanding of void-void and void-crack coalescence and void nucleation, and some criteria and models for these are discussed. The implications of the finite element results for fracture criteria based on critical stress, strain or both is discussed with respect to transition of fracture mode and the angle of initial crack growth. Localization of flow is discussed as a possible fracture model and as a model for void-crack coalescense.

---

* This is a chapter of the author's Ph.D. thesis at Brown University, June 1977. The section has already been issued as Technical Report E(11-1)3084/44, Division of Engineering, Brown University, Providence, Rhode Island, May 1976.

II. PATH DEPENDENCE OF THE J-INTEGRAL AND THE ROLE OF J AS A PARAMETER CHARACTERIZING THE NEAR TIP FIELD *

Abstract The J-integral has significant path dependence immediately adjacent to a blunted crack tip under small scale yielding conditions in an elastic-plastic material subject to mode I loads and plane strain conditions. Since the J-integral, evaluated on a contour remote from the crack tip, can be used as the one fracture mechanics parameter required to represent the intensity of the load when small scale yielding conditions exist, J retains its role as a parameter characterizing the crack tip stress fields, at least for materials modelled by the von Mises flow theory. Some results obtained using both the finite element method and the slip line theory are suggestive of a situation in which an outer field parameterized by a path-independent value of J controls the deformation in an inner or crack tip field in which J is path dependent. The outer field is basically the solution to the crack problem when large deformation effects involved in the blunting are ignored. Thus, the conventional small strain approaches in which the crack tip deformation is represented by a singularity have been successful in characterizing such features as the crack tip opening displacement in terms of a value of the J-integral on a remote contour. An interesting deduction concerns a non-linear elastic material with characteristics in monotonic stressing similar to an elastic-plastic material. Since J is path independent everywhere in such a material, the stress and strain fields near the crack tip in such a material must differ greatly from those arising in the elastic-plastic materials so far studied. This result is of significance because it is believed that such non-linear elastic constitutive laws can represent the limited strain-path independence suggested by models for plastic flow of polycrystalline aggregates based on crystalline slip within grains.

* This is a chapter of the author's Ph.D. thesis at Brown University, June 1977.

INTRODUCTION

The utility of the J-integral (Rice [1]) in fracture mechanics would seem to depend on its role as a parameter characterizing the near tip field. If the value of J, computed on a contour remote from the crack tip, directly controls the near tip stress and strain distribution and magnitudes before the onset of fracture, then J can be used to characterize the mechanics of fracture initiation. Apart from linear elastic materials, the most obvious cases in which J parameterizes the near tip field are power law hardening deformation plastic materials as analyzed by Rice and Rosengren [2] and Hutchinson [3]. In these cases, the crack tip is modelled as a singular point for strain. The strength of the singularity is determined by the hardening characteristics and the amplitude of the singularity is controlled by the path independent J. The angular characteristics of the stress and strain fields are basically determined by the hardening characteristics.

These analyses would seem to be quite accurate models for the near tip behavior in incrementally plastic materials. Thus, the near tip strain in incrementally plastic materials has a singular behavior dependent on the hardening characteristics of the material, which also sets the angular stress and strain distribution. The amplitude of the singularity is governed by a value of the J-integral evaluated on a contour shrunk onto the tip. Since there is no guarantee of path-independence of J in incrementally plastic materials, there would seem to be no certainty that a value of J computed on a remote contour would control the near tip stress and strain state in these materials. If, however, the tip value of J were equal to the remote value, i.e., path-independence of J actually does occur, or if the tip value were some constant function of

the remote value, then the near tip field would be characterized by a remote value of J. According to the small strain finite element analyses of Rice and Tracey [4] and Tracey [5] using singular crack tip elements and flow theory plasticity, the J-integral is path-independent, at least under conditions of small scale yielding. There is some uncertainty in this work concerning the path-dependence of J in the crack tip elements. However, Parks [10] has analyzed the same problems by the same methods, but using a deformation theory of plasticity. He also found J to be path-dependent in the crack tip element, despite the non-linear elastic constitutive law he used. In view of this, it would seem that there is a defect in the crack tip element as far as path-independence of J in the deformation theory is concerned. This does not rule out the possibility of a path dependence of J very close to the crack tip in the flow theory materials when conventional small strain assumptions are made. However, according to the results of Rice and Tracey [4,5], if J is path-dependent, the tip value of J is a numerical constant times the remote value of J, at least in small scale yielding. The results for small scale yielding are, in general, in agreement with the well known, one parameter characterization of fracture initiation that is the plane strain fracture toughness.

However, a recent finite element study of the blunting of crack tips in elastic-plastic materials in small scale yielding by McMeeking [6] has revealed a significant path dependence of J very close to the crack tip, on contours of radius comparable in size to a few times the crack tip opening displacement. There would seem to be no functional dependence of the tip J values on the remote J values. Indeed, the tip value would appear to be zero. If the one parameter characterization of the initiation

of fracture in small scale is dependent on the remote value of the J-integral controlling the tip value of the J-integral, and on this in turn controlling the tip stress and deformation state, then one parameter characterization of the initiation of fracture in small scale yielding should not work. It would appear, however, that an outer field, characterized by a path-independent value of J, controls the deformation in an inner, or crack tip field in which J is path dependent. Thus, the remote value of J parameterizes the near tip field while the tip value of J is possibly zero.

The comments about the flow theory materials have been restricted to the case small scale yielding. The more important questions about the role of J as a parameter characterizing the near tip field concern the cases of large scale yielding and fully plastic conditions as has been investigated by Begley and Landes [12]. With continuous hardening, as in a power law hardening material, it seems likely that a characteristic near tip field, similar to the Hutchinson [4], Rice-Rosengren [3] near tip field, arises, at least when conventional small strain assumptions are used. Since this field is dependent on the tip value of the J-integral, it would be of value, as far as characterizing fracture initiation is concerned, to understand the way the tip value of J depends on the remote value of J in flow theory materials in conditions of large scale yielding or full plasticity. If there is no hardening at all, there is known to be a gross non-uniqueness of crack tip stress and deformation fields in full plasticity of flow theory materials, as illustrated by the slip line solutions discussed by McClintock and Irwin [9]. In terms of the analysis of the mechanics of fracture initiation, it is desirable to know how soon beyond small scale yielding conditions the non-uniqueness

sets in. Once the non-uniqueness arises, it is impossible for the J-integral to uniquely characterize fracture initiation. Similarly, it is desirable to understand the relationship between fully plastic solutions for non-hardening materials and solutions for materials which have some hardening, but which eventually experience a saturation to a constant flow stress after large strain.

DEFINITION OF THE J-INTEGRAL

In view of the large deformations which occur near the tip of a blunted crack, it is necessary to define the J-integral, following Eshelby [13], as

$$J = \int_{\Gamma} \left[W dX_2 - \underset{\sim}{T} \cdot \frac{\partial \underset{\sim}{u}}{\partial X_1} ds \right] \quad , \tag{1}$$

where Γ is a path in the undeformed state of the material from the bottom surface of the notch through material to the upper surface of the notch, $\underset{\sim}{X}$ is the position of a material point in the undeformed configuration, $\underset{\sim}{u}$ is displacement, $\underset{\sim}{T} = \underset{\sim}{n}.\underset{\sim}{t}$ where $\underset{\sim}{n}$ is the outward normal to the integration path and $\underset{\sim}{t}$ is the nominal (1st Piola-Kirchhoff) stress tensor as in $t_{ij} = |F| \sigma_{pj} \partial X_i / \partial x_p$, where $|F|$ is the ratio of the volume of a material element in the deformed state to its volume in the undeformed state, $\underset{\sim}{\sigma}$ is the true stress and $\underset{\sim}{x} = \underset{\sim}{u} + \underset{\sim}{X}$. In addition, ds is an element of path length and

$$W = \int_0^{\partial u_i / \partial X_j} t_{ji} d(\partial u_i / \partial X_j) \quad .$$

Note that the definition of W means that it can also be expressed as

$$\int_0^{t_f} |F| \sigma_{ij} D_{ij} dt \quad ,$$

where t is a loading parameter which is zero in the undeformed configuration and t_f in the deformed state for which W is to be computed. The tensor $\underset{\sim}{D}$ is the rate of deformation tensor with components given by

$$D_{ij} = \frac{1}{2} (\partial v_i / \partial x_j + \partial v_j / \partial x_i) \quad ,$$

where $\underset{\sim}{v}$ is velocity. The explicit loading history of the material point for

which W is to be calculated is used in the computation, although this requirement becomes immaterial in a non-linear elastic material. The J-integral is path independent in elastic materials when defined according to (1). The definition of J coincides with the usual small strain definition when the difference between deformed and undeformed configurations can be neglected.

PATH DEPENDENCE OF THE J-INTEGRAL

Path dependence of the J-integral was detected when a finite deformation analysis of plane strain notch tip opening with contained yielding was carried out using the finite element method [6]. A notch with a semi-circular tip was opened up until the width of the notch at the tip, b, was about five times b_o, the undeformed width of the notch. The J-integral was computed on various contours around the notch tip at several levels of notch tip opening. The results are plotted in fig. 1, in which J_∞ is the value of the J-integral computed on a contour remote from the crack tip. As indicated in the figure, the results are for three, Prandtl-Reuss type, elastic-plastic materials with the same ratio of yield stress in tension, σ_o, to Young's modulus, E. The materials, however, have differing hardening properties as characterized by N. The term N is the hardening exponent in a power law hardening relationship of the form

$$(\bar{\tau}/\sigma_o)^{1/N} = \bar{\tau}/\sigma_o + 3G\bar{\varepsilon}^p/\sigma_o \quad ,$$

where $\bar{\tau}^2 = \frac{3}{2}\tau'_{ij}\tau'_{ij}$, $\underset{\sim}{\tau}'$ is the Kirchhoff stress deviator, $\underset{\sim}{\tau} = |F|\underset{\sim}{\sigma}$, G is the elastic shear modulus and $\bar{\varepsilon}^p = \int\left(\frac{2}{3}D^p_{ij}D^p_{ij}\right)^{1/2}dt$, where $\underset{\sim}{D}^p$ is the plastic part of $\underset{\sim}{D}$. The non-hardening material has $N = 0$.

As can be seen in fig. 1, the J-integral is only significantly path dependent when the contour is less than about 5 deformed notch widths from the notch tip. Indeed, further from the notch tip than about 10 current notch widths, J is path-independent. The value of J in this area of

path independence is J_∞ and the current notch width has been shown as a function of J_∞ for each material in fig. 2. A very approximate fit to the lines in fig. 2 is

$$J_\infty = (b-b_o)f_N\sigma_o \quad , \qquad (2)$$

where b is greater than about $2b_o$. The term f_N is a non-zero constant chosen to match the gradient of the line for each hardening material; ($f_o = 1.8$, $f_{.1} = 2.4$ and $f_{.2} = 3.7$).

On the other hand, the values of J in fig. 1 for $R/b < 0.5$ are very dependent on path. It would appear that a very rough fit to the results for $J/J_\infty < 0.5$ is

$$J_i/J_\infty = \ell n(b/b_o)/[(b/b_o-1)f_o] \quad , \qquad (3)$$

where J_i is just a value of J very close to, but not on, the crack tip surface, and $R = .66b_o$ for all the points with $J/J_\infty < 0.5$. Presently, there will be an attempt to give some physical basis for this result. Firstly, attention will be paid to the implications of the result for very large values of b/b_o.

An important feature of the finite element solution is that for values of b/b_o larger than about 3, a self-similar sequence of solutions develops. This is reflected in the fact that fig. 3, a plot of the near tip stress and deformation states for one particular material, is based on results from several steps of deformation. The crack tip similarly develops into a steady state shape and the influence of the original shape becomes negligible. As a result, when b/b_o is sufficiently large, the solution serves as an approximation to the smooth blunting of a sharp crack in an elastic-plastic material in contained yielding conditions.

In particular, if the solution for the opening of the notch were processed to arbitrarily large amounts of opening, the approximation could, presumably, be driven arbitrarily close to the solution for the sharp crack. If opening the notch to 5 times its original width is sufficient to indicate the trend as $b/b_o \to \infty$, then the limit of (3) as $b/b_o \to \infty$ would seem to give the solution for the tip value of J for a sharp crack. It is simple to see from (3) that

$$\lim_{b/b_o \to \infty} J_i/J_\infty = 0 \quad .$$

The characteristic length in the self similar solution is b. However, according to (2), $b = b_o + (J_\infty/\sigma_o)f_n$. It seems reasonable to use this relationship with $b_o = 0$ as the relationship between J_∞ and b for an originally sharp crack (McMeeking [6]). Thus, the length J_∞/σ_o is a length parameter which characterizes the stress and deformation field around a blunted crack tip, even although the tip value of the J-integral seems to be zero.

PATH DEPENDENCE OF THE J-INTEGRAL IN A RIGID-PLASTIC MODEL

As a confirmation of the path dependence of J, the rigid-perfectly plastic, deeply cracked, double edge-notched, thick specimen was studied using slip line theory. There is no unique flow field for this specimen. The field of slip lines and the state of stress near the crack tip is unique, however, and is shown in fig. 4. The term τ_o is the flow stress in shear and $\tau_o = \sigma_o/\sqrt{3}$. The field of displacements chosen from among the non-unique flow fields for this specimen is shown in fig. 5. This field was chosen because there are no discontinuities of velocity at the slip line separating A and C, and C and B. This means that with respect to this and to the near tip stress field, the left-hand notch experiences the same conditions as the notch in small scale yielding analyzed through the slip line method by Rice [1]. The velocities near the tip in the fans above and below the left-hand notch in the fully plastic double edge notched panel are not the same as the velocities near the tip deduced by Rice for the crack in small scale yielding. However, the velocities are not very different, and the results of a contour integral calculation of J very close to the tip in the double edge notched panel will be of some relevance to the result for small scale yielding. Notable features of the strain field chosen for the double edge notched panel are that the regions A, B, D and E are non-deforming and there is a tangential velocity discontinuity at the slip line between B and E.

At the scale of figs. 4 and 5, the details of the notch tip are obscured. This would be so as long as $b/a \ll 1$, where a is the ligament between the notch tips. Attention is henceforth restricted to values of Δ/a small enough for this to remain true. It then

follows that there are negligible differences between the deformed and undeformed positions of material points near the top of fan C. Thus, the conventional small strain definition of the J-integral may be used on a circular contour near the top of the fan. Following Rice's [14] calculation of J in this flow field, the value of J around the left-hand notch tip on a contour remote from the tip is

$$J_\infty = 2(2+\pi)\tau_o \Delta \quad . \tag{4}$$

In order to compute J on a contour on the notch tip, we need the details of the slip line field around it as given by Rice and Johnson [7]. The details are shown in fig. 6. On the scale of fig. 6, fan C is non-centered and area B is not adjacent to the notch tip. Adjacent to the notch tip is a region of spiral slip lines, in which intense strains occur. The normal velocity on the slip lines from S to the notch tip is just the radial velocity in the fan C, and so is $\dot{\Delta} \sin\theta$. Using this boundary condition, Rice and Johnson solved the slip line equations numerically for the displacements on the notch tip in terms of Δ and the original notch shape. In particular, the equivalent plastic strains $\bar{\varepsilon}^p$ on the notch tip can be computed.

The definition of the J-integral on a contour on a semi-circular notch tip of diameter b_o is

$$J_{tip} = \frac{b_o}{2} \int_{-\frac{\pi}{2}}^{\frac{\pi}{2}} W(\theta)\cos\theta \, d\theta \quad , \tag{5}$$

where θ is the polar angle from the X-axis, based on an origin at the centre of the undeformed semi-circular notch tip. For a rigid-perfectly plastic von Mises type material, $W = \sqrt{3}\,\tau_o \bar{\varepsilon}^p$. Using the

equivalent plastic strains on an originally semi-circular notch tip from the Rice and Johnson solution, a value J_{tip} for the J-integral on the notch tip may be computed. For example, when $b = 5b_o$, $J_{tip} = 3.771\tau_o b_o$. Noting that $\Delta = (b-b_o)/4$, J_∞ is seen to have a value of $10.283\tau_o b_o$ when $b = 5b_o$, and $J_{tip}/J_\infty = .367$. As b/b_o is increased, the value J_{tip}/J_∞ drops. In addition, the ratios are similar to the results for J_i/J_∞ obtained by finite elements at the same b/b_o, although allowance has to be made for the fact that the contour for J_i did not lie on the tip. As before $J_{tip}/J_\infty \to 0$ as $b/b_o \to \infty$, but this condition is subject to $a/b \to \infty$.

A feature of the solution is that the shape of the notch tip can be obtained from the shape of a sharp crack blunted by the same amount, Δ, by adding the original notch shape to the sharp crack blunted shape. This procedure is equivalent to the superposition in Henky nets, discussed by Hill [8]. As a result, the solution for the blunt notch approaches the solution for the sharp crack arbitrarily closely as b/b_o is made arbitrarily large. The solution for the originally sharp crack is a sequence of self-similar states in which all lengths scale according to b (Rice and Johnson [7]). For example, the point S lies $1.9b$ from the crack tip surface. Since $b = 4\Delta$ in the case of an originally sharp crack, it follows that in the self-similar solution all lengths scale by J_∞/τ_o, or equivalently J_∞/σ_o. As before, the value of J on a remote contour characterizes the near tip field, while J_{tip} seems to be zero.

Of course, these comments concerning J as a characterizing parameter in fully plastic rigid-plastic materials must be treated with care. In the right-hand notch in fig. 5, the contributions to the

J-integral arise entirely from the discontinuities in displacement between B and E. The value of J-integral on a remote contour is, as before, $2(2+\pi)\tau_0\Delta$. However, the flow field around this notch tip is very different from that around the left-hand notch tip, so J_∞ only characterizes the left-hand notch from one state of deformation to another in the given flow field. It does not necessarily characterize one notch as compared to another. For example, a single edge notch in a fully plastic specimen would even have a different stress state at the notch tip compared with the double edge notched specimen (McClintock and Irwin [9]). This difficulty is not present in the small scale yielding of elastic-plastic materials. Since the rigid-plastic model is the limiting behavior of an elastic-plastic material, the question of the extent to which J_∞ **uniquely** characterizes the deformation and stress around any notch as small scale yielding conditions are exceeded is important to J-fracture toughness testing.

CRACK AND NOTCH TIP BLUNTING

It would seem that when a proper account is taken of the blunting of crack or notch tips, a path dependence of the J-integral can be detected. This is illustrated quite readily by the rigid-plastic model so far discussed. If the crack or notch tip is modelled by a point centering fans carrying singular shear strains above and below the tip, then the J-integral is path-independent all the way into the crack or notch tip. This would apply to the rigid-plastic model with the flow field given by fig. 5, and this type of field is discussed in a more general way by Rice [1]. However, when the analysis takes account of blunting, as in the work of Rice and Johnson [7] and illustrated in fig. 6, the path dependence of J is detected. The path dependence of J would seem to be associated with the area near the blunted crack tip in which large strains occur. This inner field of large deformations is surrounded by the outer field, as deduced using the crack tip as a point of singlular strain. The J-integral is path-independent in the outer field, as long as the contour on which it is computed is sufficiently far away from the crack tip. Note that so far no analysis has been carried out in the region between remote contours and crack tip contours in the rigid-plastic model.

The same features of inner and outer field are present in the finite element results concerning blunting of a notch tip with contained yielding (McMeeking [6]). Sufficiently far away from the notch tip, the stresses and deformations become similar to those deduced by Rice and Tracey [4] and Tracey [5] for the same problem. They modelled the crack tip as a singular point for strain, using special crack tip

finite elements. Parks [10] has noted that the J-integral was path-independent in the solutions of [4 and 5] except in the crack tip elements. However, this path dependence of J in the crack tip element persisted when a deformation plastic material was analyzed, suggesting that the path dependence was a defect in the crack tip singular element.

Path dependence of J arises in the region of intense deformations near the notch tip in the solution of notch blunting by finite elements, and J becomes path-independent away from the notch tip in the region of the solution where the Rice and Tracey results are approached.

These results are suggestive of a situation in which an outer field in which J is path-independent with value J_∞ controls the deformation on an inner field in which J is path dependent. The outer field is basically the solution to the crack problem when large deformation effects involved in the blunting are ignored. For this reason, the approaches to crack problems such as those of those of Rice [1] for non-hardening deformation plastic materials, Rice and Rosengren [2] and Hutchinson [3] for deformation, plastic power law hardening materials, Rice and Tracey [4] for non-hardening elastic-plastic materials and Tracey [5] for power law hardening elastic-plastic materials, have been successful in characterizing, say, the crack tip opening displacement in terms of a value of the J-integral on a remote contour, although they ignore the effect of blunting.

DEFORMATION NEAR NOTCH TIPS IN INCREMENTAL AND DEFORMATION THEORY MATERIALS

We have noted that in the incremental theory of elastic-plastic materials, a path dependence of the J-integral can arise at the notch tip. However, no such path dependence of J can arise in a deformation theory, since these materials are actually non-linear elastic. This implies some difference between the crack tip deformations of these two materials.

If the stretch ratio tangential to the notch tip surface of material lying on the notch tip surface is λ, then W is approximately $2\sigma_o(\ell n\lambda)/\sqrt{3}$ after strains large compared to yield and dilational strain have accumulated on the notch tip in a non-hardening material. This applies to both the incremental and deformation theories of plasticity. It follows from (5) that

$$J_{tip} = \frac{b_o\sigma_o}{\sqrt{3}}\int_{-\frac{\pi}{2}}^{\frac{\pi}{2}} \left[\ell n\lambda(\theta)\right]\cos\theta\, d\theta \qquad (6)$$

on a contour lying on the tip of an originally semi-circular notch of diameter b_o.

Recalling from (2) and (3) that in an incremental theory the value of the J-integral on a contour close to the crack tip in a non-hardening material seems to be approximated well by

$$J_i = b_o\sigma_o\, \ell n(b/b_o) \qquad (7)$$

when b/b_o is sufficiently large, we note that if (7) applies approximately to the contour on the notch tip, then

$$\int_{-\frac{\pi}{2}}^{\frac{\pi}{2}} \left[\ell n\lambda(\theta)\right]\cos\theta\, d\theta \approx \sqrt{3}\, \ell n(b/b_o) \quad .$$

One way in which this relationship could arise is if $\lambda(\theta)$ were equal to b/b_o everywhere on the notch tip; the approximation would then involve the difference between 2 and $\sqrt{3}$. Indeed, the true strains on the notch tip in the finite element solution seem to agree very roughly with this, being about $\ell n(b/b_o)$ at $\theta = 0$ and falling to $1/2\ \ell n(b/b_o)$ at $\theta = \pi/2$.

Turning now to the deformation theory material, we note that the J-integral must be path-independent, and according to the finite element results, eqn. (2) the value would seem to be $1.8(b-b_o)\sigma_o$ for the non-hardening material when b/b_o is sufficiently large. Of course, this value for J was computed on a contour remote from the notch tip in an incremental theory material. However, the experience of Parks [10] in comparing the deformation theory with the incremental theory in the outer field is that the deformations and stresses are the same. Hence, we will assume that the value of J in the outer field of the analysis <u>including</u> the effects of blunting will be given by (2). This value is equated with the expression for J on a contour on the notch tip, and so

$$\int_{-\frac{\pi}{2}}^{\frac{\pi}{2}} \left[\ell n\lambda(\theta)\right]\cos\theta\, d\theta \approx 3.12\ (b/b_o - 1) \quad .$$

Thus, the notch tip strains in the deformation theory material must differ from those of the incremental theory material. In addition, the strains on the notch tip in both materials must be compatible with the opening ratio b/b_o.

This result for deformation plastic materials is important, because of the relationship between deformation theory plasticity and models for

polycrystalline multi-slip during almost radial straining. For example, the model of Batdorf and Budiansky [15] leads to an exact equivalence with deformation theory under moderately non-radial loading. In this model, the strain rate of the polycrystal is computed as the average, over all orientations, of the strain rate in a single crystal subject to the macroscopic stress state. On the other hand, the self-consistent model of Hutchinson [11] leads to an approximate equivalence with deformation theory. In this model, individual crystals are modelled as spheres lying within homogeneous material which has the net constitutive properties of the polycrystal. The stress state in the polycrystal is computed as the average stress rate in the crystal over all orientations of crystal relative to the homogenous material. Applying this self-consistent model to uniaxial tensile stressing of an elastically isotropic, non-hardening, polycrystalline, fcc material, Hutchinson found that the moduli for subsequent increments of shear strain fall as strain is accumulated. In an incremental macroscopic theory for plasticity, the moduli for increments of shear strain due to uniaxial stress are constant. This is because a shear strain rate is tangential to the yield surface representing a state of uniaxial stress. In the polycrystalline model, Hutchinson found that the drop in the moduli for subsequent shear strains is approximated well by the appropriate moduli in a deformation theory of plasticity.

These models imply a deformation theory constitutive law only when the loading is at the most moderately non-radial. But near the blunting crack tip there can be very non-radial loading. However, it seems reasonable to assume that the polycrystalline models for slip will lead to a macroscopic flow theory somewhat intermediate to von Mises flow theory and deformation plasticity.

In that case, the near tip deformations would be significantly differen from those already worked out for an incremental theory of plasticity by McMeeking [6] and Rice and Johnson [7].

ACKNOWLEDGEMENT

The author is indebted to Professor J. R. Rice for helpful discussions of this topic. The author received support from the U. S. Energy Research and Development Administration under contract E(11-1)3084 and from the N. S. F. Materials Research Laboratory to carry out this work.

REFERENCES

1) Rice, J.R., Journal of Applied Mechanics, Vol. 35, 1968, pp. 379-386.

2) Rice, J.R., and Rosengren, G.F., Journal of the Mechanics and Physics of Solids, Vol. 16, 1968, pp. 1-12.

3) Hutchinson, J.W., Journal of the Mechanics and Physics of Solids, Vol. 16, 1968, pp. 13-31.

4) Rice, J.R., and Tracey, D.M., in Numerical and Computer Methods in Structural Mechanics, S.J. Fenves et al., Ed., Academic Press, New York, 1973, pp. 585-623.

5) Tracey, D.M., Transactions ASME (Series H, Journal of Engineering Materials and Technology), Vol. 98, 1976, pp. 146-

6) McMeeking, R.M., "Finite deformation analysis of crack tip opening in elastic-plastic materials and implications for fracture initiation," Technical Report E(11-1)3084/44, Division of Engineering, Brown University, Providence, Rhode Island, May 1976.

7) Rice, J.R., and Johnson, M.A., in Inelastic Behavior of Solids, M.F. Kanninen et al., Ed., McGraw-Hill, New York, 1970, pp. 641-670.

8) Hill, R., Journal of the Mechanics and Physics of Solids, Vol. 15, 1967, pp. 255-

9) McClintock, F.A., and Irwin, G.R., In Fracture Toughness Testing and Its Applications, STP 381, American Society for Testing and Materials, Philadelphia, 1965, pp. 84-113.

10) Parks, D.M., "Some Problems in Elastic-Plastic Finite Element Analysis of Cracks," Ph.D. Dissertation, Brown University, Providence, Rhode Island, 1975.

11) Hutchinson, J.W., Proceedings of the Royal Society, Series A, Vol. 319, 1970, pp. 247-272.

12) Begley, J.A., and Landes, J.D., in Fracture Toughness, STP 514, American Society for Testing and Materials, Philadelphia, 1972, p. 1.

13) Eshelby, J.D., in Inelastic Behavior of Solids, M.F. Kanninen et al., Eds., McGraw-Hill, New York, 1970, p. 77.

14) Rice, J.R., in Mechanics and Mechanisms of Crack Growth, Proceedings of April 1973 Conference, Cambridge, M.J. May, Ed., British Steel Corporation, Physical Metallurgy Center Report, 1975, p. 14.

15) Batdorf, S.B., and Budiansky, B., Journal of Applied Mechanics, 21, 1954, p. 323.

List of Figure Captions

Figure 1 Plot of J-integral, computed from the finite element results for the blunting of a notch with contained yielding, versus the distance from the notch tip of the contour on which J is calculated.

Figure 2 Plot of notch width, b, versus the value of the J-integral, J_∞, computed on a remote contour around the notch tip.

Figure 3 Plot of stress $\sigma_{\theta\theta}/\sigma_o$ and plastic strain around the blunted notch for $\sigma_o/E = 1/300$ and $N = 0$. Note σ_o is the yield stress in tension and R and θ are defined for the position of the material in the undeformed configuration.

Figure 4 Near tip stress state and slip lines for rigid-plastic model.

Figure 5 Displacements for rigid-plastic model.

Figure 6 Slip line field around a blunt notch with velocities in C corresponding to the left hand notch in fig. 5.

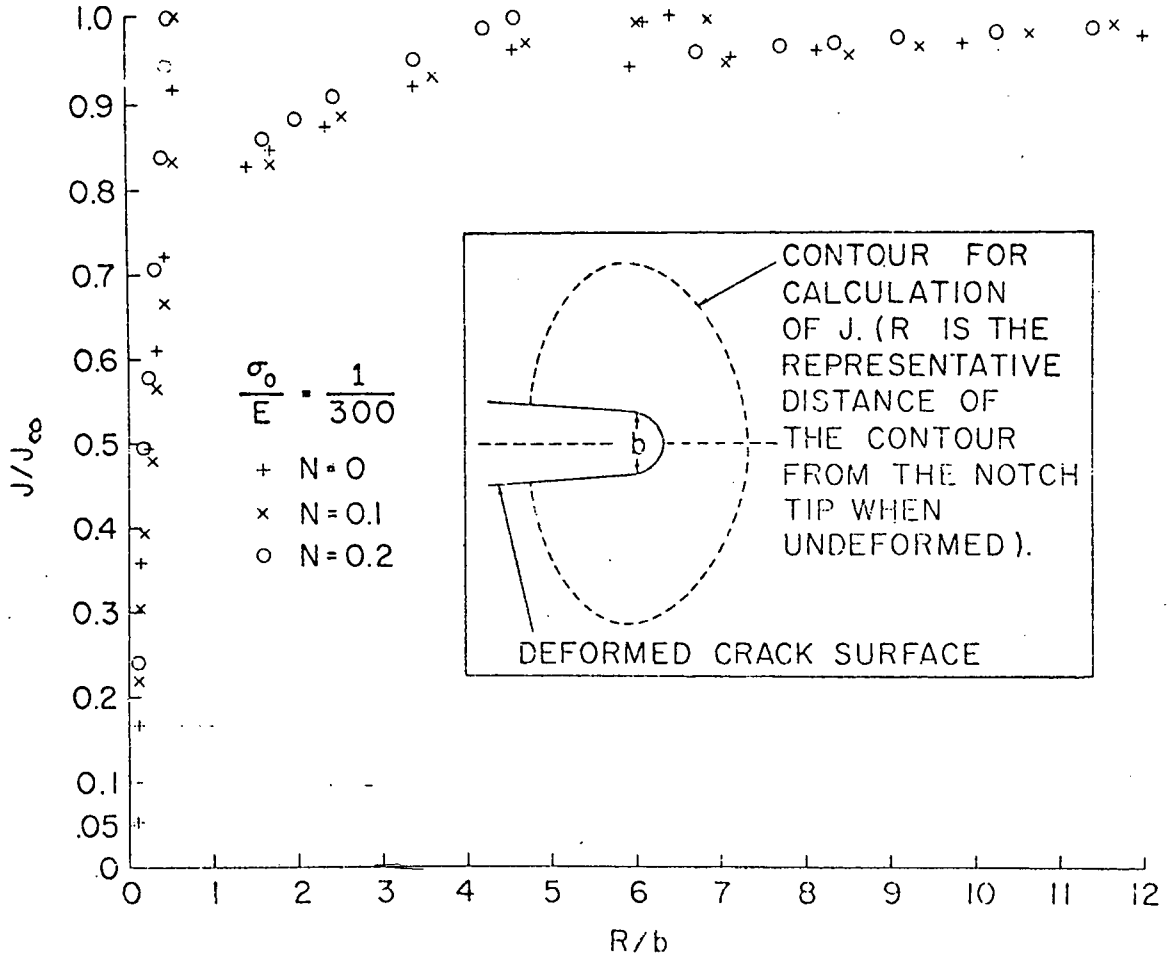
1.0
0.9
0.8
0.7
0.6
0.5
0.4
0.3
0.2
0.1
.05
0
J/J∞
0 1 2 3 4 5 6 7 8 9 10 11 12
R/b
σ0/E = 1/300
+ N=0
× N=0.1
○ N=0.2
b
CONTOUR FOR CALCULATION OF J. (R IS THE REPRESENTATIVE DISTANCE OF THE CONTOUR FROM THE NOTCH TIP WHEN UNDEFORMED).
DEFORMED CRACK SURFACE

Figure 1

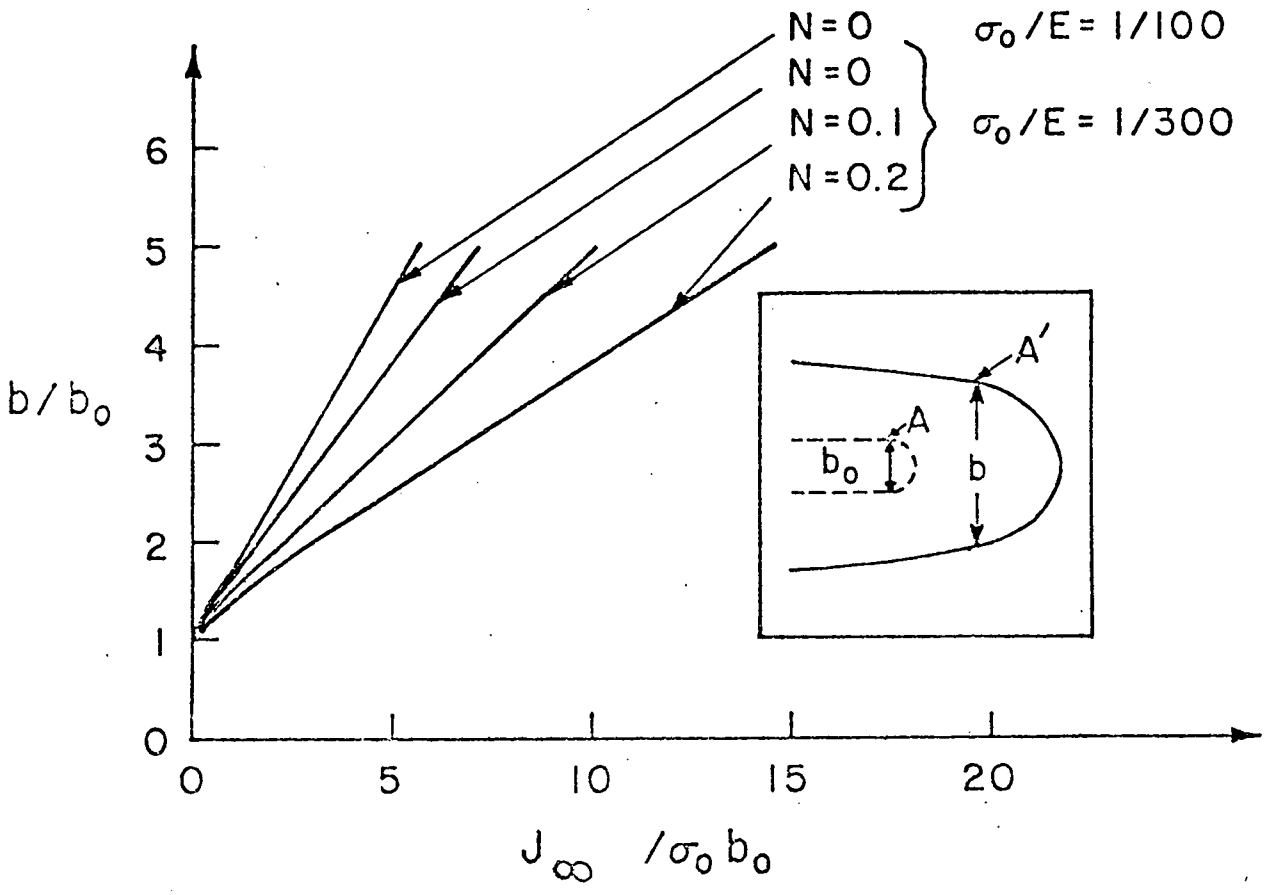
N = 0
N = 0
N = 0.1
N = 0.2
σ0/E = 1/100
σ0/E = 1/300
A'
A
b0
b
b/b0
0
1
2
3
4
5
6
0
5
10
15
20
J∞ /σ0 b0

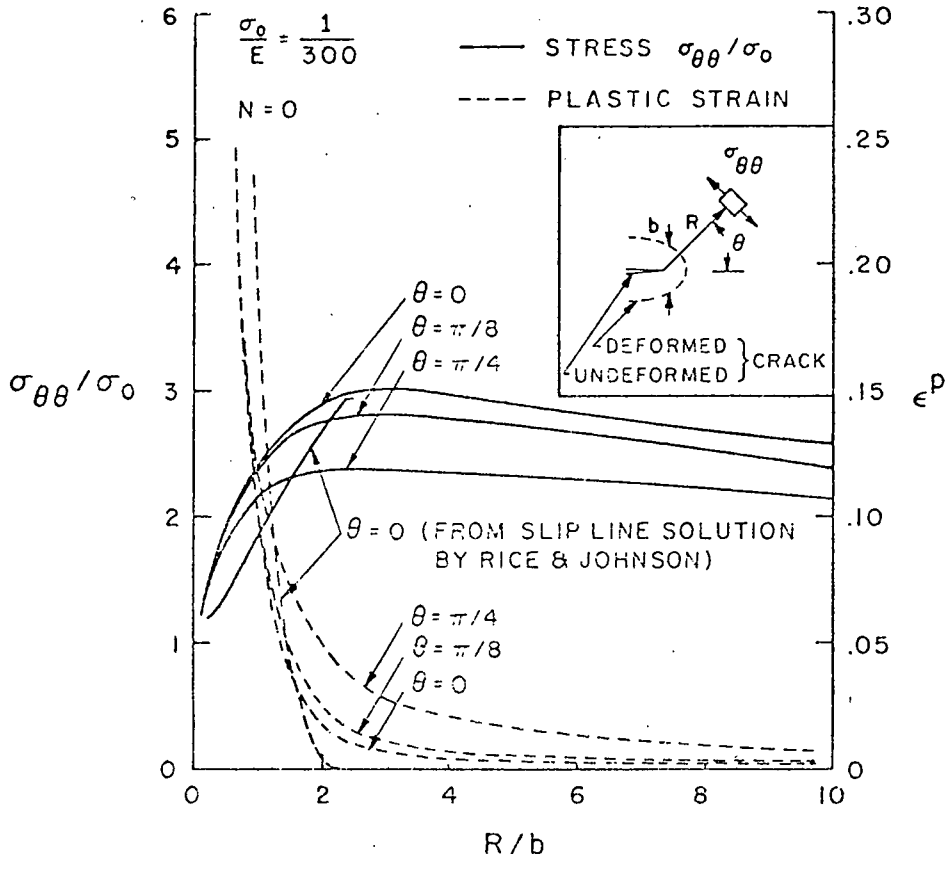
$\frac{\sigma_0}{E} = \frac{1}{300}$
N = 0
STRESS $\sigma_{\theta\theta}/\sigma_0$
PLASTIC STRAIN
$\sigma_{\theta\theta}$
b
R
θ
DEFORMED
UNDEFORMED
CRACK
θ = 0
θ = π/8
θ = π/4
θ = 0 (FROM SLIP LINE SOLUTION BY RICE & JOHNSON)
θ = π/4
θ = π/8
θ = 0
$\sigma_{\theta\theta}/\sigma_0$
ϵ^p
R/b
0
1
2
3
4
5
6
0
2
4
6
8
10
.05
.10
.15
.20
.25
.30

Figure 3

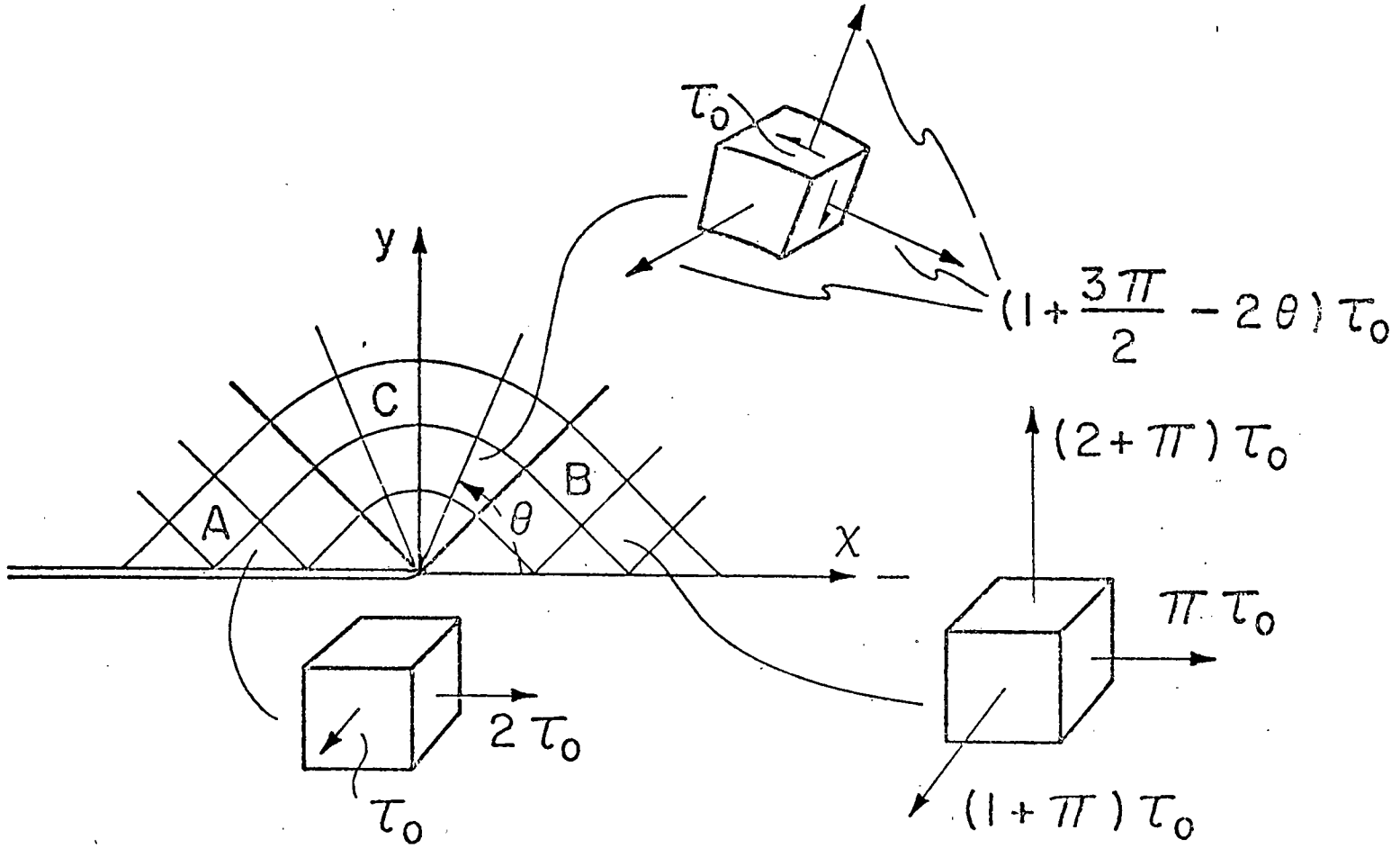
τ_0
y
$(1+\frac{3\pi}{2}-2\theta)\tau_0$
C
$(2+\pi)\tau_0$
B
A
θ
X
$\pi\,\tau_0$
$2\tau_0$
τ_0
$(1+\pi)\tau_0$

Figure 4

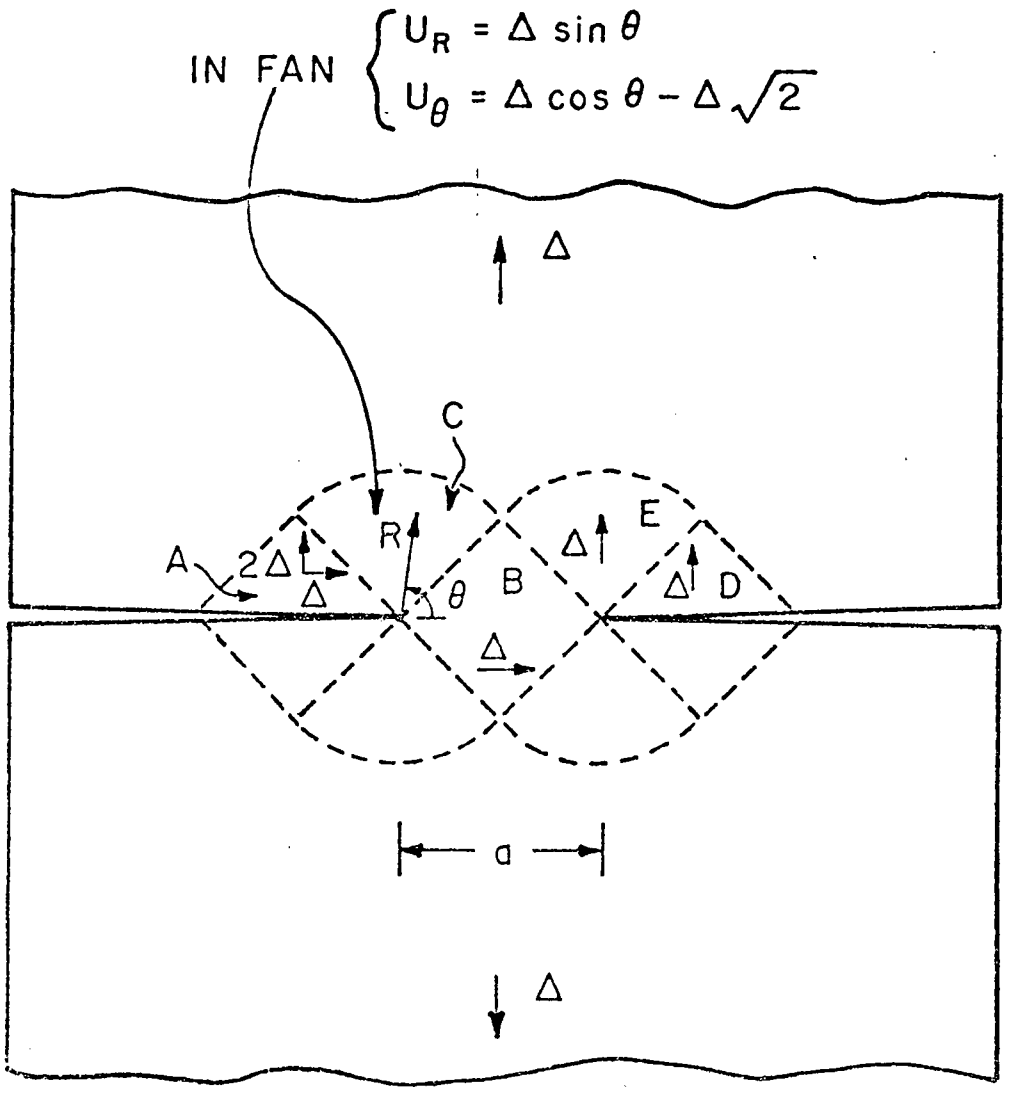
IN FAN
$U_R = \Delta \sin\theta$
$U_\theta = \Delta \cos\theta - \Delta\sqrt{2}$
Δ
C
R
A
2Δ
Δ
θ
B
Δ
E
Δ
D
Δ
a
Δ

Figure 5

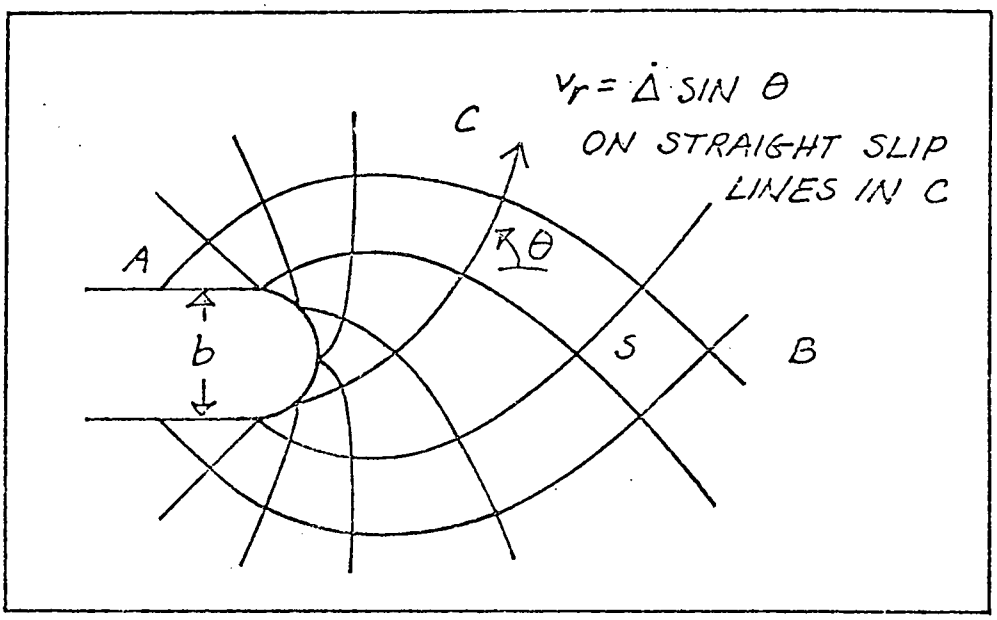

Figure 6

III SEPARATION ENERGY RATE FOR A FINITE CRACK GROWTH STEP FROM A BLUNTED MONOTONICALLY LOADED CRACK TIP IN AN ELASTIC-PLASTIC MATERIAL *

Summary The energy released by relaxing simultaneously to zero the tractions on the new surface created by a finite step of crack growth from a loaded blunt crack in an elastic-plastic material has been calculated using a finite element method suitable for large deformations. The energy released per unit length of crack growth is non-zero when the unloading occurs in this manner, in contrast to continuous crack growth in elastic-plastic materials, where the energy release rate is zero. The trend of the finite element results for the energy release rate for finite growth steps is in agreement with the zero energy release rate for continuous crack growth. The growth steps in the current investigation are of order a few times the crack tip opening displacement at the onset of growth, at the end of the monotonic loading, and are smaller compared to plastic zone dimensions than the growth steps studied in previous work [1,2]. The results agree quite well with the calculations for initial growth step in this previous work. Although most of the results here are for the initial growth step, some calculations were carried out for subsequent growth steps. The energy release rate for subsequent growth steps differs from that for the initial growth step. This is discussed in the context of the stress state prior and subsequent to crack growth.

---

* This is a chapter of the author's Ph.D. thesis at Brown University, June 1977.

INTRODUCTION

A paradox arises when a Griffith-type energy balance is applied to continuous crack growth in an elastic-plastic material with a stress-strain relationship which saturates to a finite flow stress at large strain. One may show that the work done by external loads during such a process equals the energy absorbed by material deformation in plastic flow [3]. In particular, no surplus energy is available for the work of separation. The essential reason for this is that there is no singularity in recoverable energy density at the crack tip in these materials. It seems likely that the paradox would arise also in a material with a power-law or linear hardening behavior with parameters typical of structural metals, and Kfouri and Miller [1] have partially confirmed this.

By using the concept of a finite fracture zone, and thus a finite crack growth step, Kfouri and Miller [1] have shown that a surplus of energy can arise at the crack tip in a material with a linear hardening law. They modelled the fracture event in a center cracked panel loaded into the plastic range by releasing the crack tip node in their finite element mesh and relaxing the force on that node to zero. This produced a finite growth step of one nodal spacing. The energy release associated with unloading the tip node allows calculation of the energy release per unit length of finite crack growth, G^{Δ}. As expected, the results indicate that in the limit of infinitesimal crack growth, $G^{\Delta} \to 0$.

However, the smallest growth step studied by Kfouri and Miller is many times the crack tip opening displacement. In that case, modelling the crack tip before fracture as a point should be quite accurate. This is because the energy released during a finite growth step of this size is associated dominantly

with material unaffected by blunting of the crack tip. However, if the finite growth step was about the same size as the crack tip opening displacement, then the crack would be growing into the material heavily affected by prior crack tip blunting. A more precise modelling of the crack tip prior to crack growth is necessary. This is available in the finite element results presented by McMeeking [7], concerning the smooth blunting of a crack in an elastic-plastic material. By allowing crack growth in the same program, it was possible to study the separation energy rate associated with growth steps which were similar in size to the crack tip opening displacement. Most of the results are for the onset of fracture and agree with the results of Kfouri et al. [1,2]. In addition some calculations were made for growth steps subsequent to fracture initiation. This computation was restricted to a series of very small steps compared to the crack tip opening displacement. In these, G^{Δ} rises with each additional growth step, in contrast to calculations by Kfouri et al. [1,2], who observed that G^{Δ} fell during subsequent growth steps. It is proposed that the difference in behavior is associated with the state of stress around a blunted crack tip, and perhaps it is inherent to the small step size or to the small amount of total growth distance covered in the program of growth steps studied here.

FINITE ELEMENT CALCULATIONS OF SEPARATION ENERGY RATE

The calculation of the separation energy rate was carried out based on the results of McMeeking [7]. He analyzed the stresses and deformations around a crack tip in an elastic-plastic material smoothly blunted open by mode I opening loads. The deformation is plane strain and the results are limited to contained yielding about the crack tip. The constitutive law used was the Prandtl-Reuss equation with a hardening law of the form

$$(\bar{\tau}/\sigma_o)^{1/N} = \bar{\tau}/\sigma_o + 3G\bar{\varepsilon}^p/\sigma_o \quad ,$$

where $\bar{\tau}^2 = \frac{3}{2}\tau'_{ij}\tau'_{ij}$, $\underset{\sim}{\tau}'$ is the Kirchhoff stress deviator, $\underset{\sim}{\tau} = |F|\underset{\sim}{\sigma}$ where $|F|$ is the ratio of volume of a material element in the current state to its volume in the undeformed state, $\underset{\sim}{\sigma}$ is the true stress tensor, σ_o is the tensile yield stress in terms of Kirchhoff stress, G is the elastic shear modulus. Note that $\bar{\varepsilon}^p = \int\left(\frac{2}{3}D^p_{ij}D^p_{ij}\right)^{1/2}dt$, where $\underset{\sim}{D}^p$ is the plastic part of the rate of deformation tensor $D_{ij} = (\partial v_i/\partial x_j + \partial v_j/\partial x_i)/2$, where $\underset{\sim}{v}$ is velocity, $\underset{\sim}{x}$ is the current material position and t is time. The particular material properties which were used for the calculation of separation energy rate were $N = 0.1$, $\sigma_o/E = 1/300$, where E is Young's modulus, and a Poisson's ratio of 0.3. The near tip stress and deformation state is shown in fig. 1, which is taken from [7].

In McMeeking's finite element calculations, the mesh was semi-circular, with the crack represented by unconstrained nodes along half of the non-circular side of the mesh. The remaining nodes on the non-circular side of the mesh, lying in front of the crack tip, were constrained to remain on an axis of symmetry for mode I loading. To carry out the separation energy rate calculations, the boundary conditions were reformulated so that the

positions of all nodes on the outer ring remained fixed. Then the constraint on the nodes to be unloaded was replaced by a force boundary condition just sufficient for equilibrium. Thereafter, the nodes were relaxed proportionatey in five increments until they transmitted no forces. The energy released by each node was computed by integrating the force-displacement record for the five increments using a trapezoidal rule. The separation energy rate, G^{Δ} , was computed by dividing the energy released by Δa , the new length of crack created. This calculation was carried out for several values of Δa . The crack growth calculations were processed with the notch already blunted open monotonically to about 5 times its original width.

Crack tip shapes after an initial step of finite growth. The initial step of growth of the crack from the blunted tip surface always involved the relaxation of four or more nodes simultaneously. Thus the shapes achieved after complete relaxation would appear to be relatively accurate records, as compared to the shapes determined by Kfouri et al. [1,2]. Since Kfouri et al. included only one node to model the crack growth initiation step and used straight-sided elements, they were limited to producing new crack surfaces in a wedge shape. Since the growth steps from the blunted crack were produced with one node representing the new crack tip, they have the same wedge shaped tip as the crack growth segments produced by Kfouri et al. However, the extra nodes along the flank produce a better fit to the shape of growth steps compared to the wedge shapes of Kfouri. A growth step, which is produced by simultaneously relaxing 9 nodes, is illustrated in fig. 2. The newly created crack has nearly parallel flanks, except near the new tip, which is modelled by one point. The original

blunted crack tip moves almost rigidly during the relaxation. Some details of the shapes of the new crack segments produced by finite growth steps are tabulated. In the table there is listed the width of the new crack at the blunted tip surface (point A in fig. 2) and at its widest point. These quantities are normalized by the length of the growth step. In addition, the growth step length is listed in units of J_{app}/σ_o , $(K/\sigma_o)^2$ and the crack tip opening displacements prior to crack growth.

The shapes of the growth steps are possibly significant to the phenomenon of the retardation of fatigue crack growth after a cycle of overload. This phenomenon has been discussed, for example, by Schijve [4]. Paris [5] has suggested that the retardation effect is produced as a result of material behind the crack tip interfering and holding the crack tip closed during load cycling subsequent to overload. For the purpose of a discussion of this idea, let the previously blunted crack tip in fig. 2 be the tip shape produced by a single cycle of tensile overload. So that an exact equivalence between the model for fatigue crack growth retardation and fig. 2 applies, assume that a finite amount of crack growth occurs at the peak of the overload cycle. This will occur with the shape as in fig. 2. When the crack is unloaded, it is likely that the crack surface near the blunt tip produced by the cycle of overload will interfere, producing the closure of the crack tip in Paris' model. When the loads are cycled at the normal level thereafter, the crack tip is open during only part of the cycle. A reduced amount of crack growth results. When the growth has proceeded sufficiently, the crack surfaces no longer interfere and the crack tip is open for more of the cycle. The situation returns to that which prevailed prior to overload and crack growth returns to its previous rate.

The assumption, that there is the occurrence of a finite amount of crack growth which is large compared to the previous cyclic growth steps, is not supported by striation measurements as made, say, by Hertzberg [8]. Rather, it appears that the crack growth after the overload is in step sizes that would be produced by the subsequent cycling. It would thus seem more likely that the interference effects are due to the closing up of the blunted crack tip produced by the overload.

Separation energy rates for an initial step of finite growth. The value of G^{Δ}/J_{app} is plotted against $S = \Delta a/(K/\sigma_o)^2$ in fig. 3 using both the results of the present study and the results presented in [2] for an initial step of growth. The term K is the stress intensity factor after monotonic loading, before any crack growth, b is the crack tip opening displacement and the distance Δa is the undeformed size of the growth step, before any load was applied to the crack. The value of J_{app} is the value of the J-ingetral (Rice [9]) on a remote contour prior to any crack growth. The plastic zone size prior to crack growth is proportional to $(K/\sigma_o)^2$ so that S is a measure of the growth step size relative to the size of the plastic zone. As can be seen, all the results follow a trend of increasing G^{Δ}/J_{app} for increasing S. It would appear that the results in fig. 3 fall into two segments. For small values of S, the value of G^{Δ}/J_{app} rises quite steeply with increasing S and appears fairly linear. At larger values of S the results rise less steeply and the gradient decreases with increasing S.

Note from fig. 1 that the stress magnitude in front of the crack rises to a peak level some distance from the blunted crack surface and then steadily falls off as one goes further from the crack tip. The peak stress lies at

approximately 2.5b from the crack tip. In the chosen configuration just prior to crack growth, $b \approx .5\ J_{app}/\sigma_o$ and thus the peak stress lies at about $.004\ (K/\sigma_o)^2$ from the crack tip. Thus the sharp change in the gradient of the results of fig. 3 takes place around about the point where the crack growth step size coincides with the distance from the crack tip to the point of peak stress. A physical explanation may be that as the crack growth step size is increased from zero up to the point of peak stress it absorbs new points which carry greater stress prior to separation than points already included in the growth step. When the growth step is extended beyond the peak stress point, each new point encompassed by the growth step is stressed to a lower level than some points already included. If the potential for energy release at a point is dependent on the traction prior to relaxation, which seems very likely, then G^{Δ}/J_{app} will rise as S increases from zero, and then change over to a less steep rise once the peak stress point is included in the growth step. No attempt is made here, however, to explain why the results in fig. 3 should form the straight line at small S. Indeed, the results do not indicate so clearly any such relationship when $\chi = J_{app}/G^{\Delta}$ is plotted against $\zeta = S\chi = (1-\nu^2)\sigma_o{}^2\Delta a(EG^{\Delta})$, as in fig. 4. The straight line corresponding to that in fig. 3 has been included. It should be noted that one result, namely (.404,1220) has been omitted from fig. 4. If it were not for this point, one might conclude that the line $\zeta = .075$ fits the results quite well for the higher values of χ in fig. 4. When plotted in the manner of fig. 4, the results of Kfouri et al. do not agree quite so clearly with the results obtained here.

In any case, some reservation must be made about putting the results of Kfouri et al. [1,2] for linearly hardening materials together with results for a power law hardening material and drawing too many conclusions. However,

the trend of the results is in agreement, and together the result would seem to indicate that $G^{\Delta}/J_{app} \to 0$ as $S \to 0$. This result is of some interest in view of the fact that the materials in this investigation and Kfouri's do not have limited flow stresses at large strains. The conclusion that elastic-plastic materials with ultimately infinite flow stresses may involve an energy release rate that is zero in continuous crack growth may be drawn. The point is by no means proved. The infinite strains at the crack tip were not modelled exactly by the finite element methods used here and by Kfouri et al. So, it would seem that the infinite flow stresses at the crack tip do not actually get into the calculations of G^{Δ}.

Stress ahead of the crack tip. The stress ahead of the crack tip both prior to initiation of finite crack growth and subsequent to crack growth for two values of Δa is shown in fig. 5. Note that X is the position of the point prior to blunting of the original crack. The two examples of the stress after crack growth shown in the figure are typical in that the stress in the element just ahead of the new crack tip is greater after crack growth than before. As can be seen, the change in the stress is not a long range effect, and at about a distance Δa beyond the new crack tip, the stress state is virtually unaltered. In the two examples shown $\Delta a/b = .21$ and 1.04, so that the crack is growing into an area of increasing stress. When the steps of crack growth are larger, the stress in the element just ahead of the new tip is still raised above its previous level. It is difficult to estimate the gradients of stress in these last cases, because the near tip element and the element beyond are too far apart to be useful. Better estimates of near tip stress gradients after crack growth could be obtained with a mesh, which is more refined just ahead of the crack growth step. This information would be useful to the better understanding

of stable cracking in hardening materials.

The new crack tip that is formed after the finite step of growth is sharp, since it is represented by a point. It acts as a point of singular strain, and, as a consequence, the stress near the crack tip is high in the power-law hardening material investigated. Rice [6] has analyzed steady-state continuous crack extension in perfectly plastic plane strain. He found that the strain is singular with strength $\log(1/r)$, where r is the distance from the moving crack tip. It seems reasonable that the strains near a crack tip produced by a finite growth step in a power-law hardening material would be similar. The stress in the element nearest the crack tip after crack growth is elevated, but the mesh is not designed well enough to give any more definite information about the near tip stress state.

Separation energy rates for a few small steps of consecutive finite growth.

In the case of the smallest initial step of finite crack growth, three further steps of finite crack growth were carried out. The growth step sizes, in units of $(K/\sigma_o)^2$, were 3.31×10^{-4}, 4.40×10^{-4}, 3.55×10^{-4}, 4.97×10^{-4}, where K is the stress intensity factor prior to any crack growth. Alternately, the step sizes were .21b, .28b, and .23b and .32b. The values for G^{Δ}/J_{app} computed for these four finite growth steps were 8.20×10^{-4}, 5.71×10^{-3}, 8.34×10^{-3} and 1.45×10^{-2} respectively. These small values reflect the fact that the step sizes are small relative even to the width of the notch. However, it is interesting that G^{Δ}/J_{app} rises consistently with each subsequent step of growth, even although the size of the finite growth step does not increase with each step of growth. The explanation seems to lie with the increasing stress level immediately in front of the monotonically loaded blunt notch tip. Each subsequent step of growth occurs into material stressed to a higher level than the material

into which the previous step grew. If, as discussed previously, the energy released is dependent on the stress level, as seems likely, G^{Δ} will rise with each new step. Once crack growth passes beyond the stress peak in front of the monotonically loaded blunt tip, then G^{Δ} could be expected to fall with each new step of growth.

When Kfouri and Miller [1] carried out a similar calculation, they found that the value of G^{Δ} fell with each new step of growth until a steady value was reached after three or four steps of growth. Their growth step sizes were many times greater than the steps for which calculations were carried out here. In the case of Kfouri and Miller's analysis, each new step of growth occurs into material stressed to a lesser degree than the material into which the previous step grew, at least based on the stress state before any growth at all. But as the crack grows, it sets up a new near tip field, basically involving the $\log(1/r)$ strain singularity previously discussed. Judging from the results of Kfouri and Miller, after a few steps of growth, this field eventually shows little dependence on the deformation and stress field that existed prior to any crack growth at all. This last point of view is based on the fact that G^{Δ} does settle down to a steady value. The very small steps of growth studied in this paper do not appear to be sufficient to establish this steady state near tip field. This may be due to the individual steps being too small, or the total amount of growth being too small. It was not possible to resolve this point because of the configuration of the finite element mesh used. Kfouri and Rice [2] constructed a model that allowed them to extrapolate the steady values of G^{Δ} in Kfouri and Miller's work for large steps of crack growth into the region of small steps of crack growth. The model

was based on the cohesive zone model of crack tip yielding, but also involved some fitting to the finite element results of Kfouri and Miller [1]. In view of the results just discussed, the model would appear not to be useful for steps of growth that are comparable in size with the crack tip opening displacement. Because of the localized effects of crack tip blunting under monotonic loading, as discussed by McMeeking [7] and not accounted for in the calculations of Kfouri and Miller, there may be some lower limit in terms of S to the extrapolation based on Kfouri and Rice's model.

CONCLUDING DISCUSSION

In discussing the physical interpretation of their results, Kfouri et al. [1,2] note that a particular feature of material behavior can be predicted. This feature is the transition of fracture mode with temperature. For simplicity, assume that Δa and G^{Δ} are fixed material parameters. This is equivalent to saying that fracture always occurs over some fixed microstructural distance and requires a given energy release rate. (As Kfouri and Rice [2] point out, Δa and G^{Δ} may be functions of temperature, but in that case, the principles of the subsequent discussion would still apply). Since Δa and G^{Δ} are fixed for a material, the parameter ζ represents the "condition" of the material, and will vary with temperature through the dependence of σ_o on temperature. Referring now to fig. 4, assume that there is some unique "fracture initiation locus" line through the results. Consider material in state $\zeta = .1$. If a specimen of this material is loaded, the value of χ will increase and fracture initiation can occur when the point $(.1,\chi)$ on the ζ,χ plane reaches the fracture initiation locus. If the material is heated so that σ_o falls and $\zeta = .05$, then no matter how much load is applied, fracture initiation cannot occur in the mode parameterized by the given values of Δa and G^{Δ}. This could correspond to the brittle-ductile transition, and it is suggested that the value for ζ at transition is about .07.

CONCLUSIONS

When crack growth occurs in a finite step of growth from a previously blunted crack in an elastic-plastic material, a non-zero separation energy release rate results. Judging from the results for various sizes of steps of initial crack growth from the blunted crack obtained using the finite element method, the energy release rate for an infinitesimal step of growth is zero. The results computed here are generally in agreement with those previously computed by Kfouri et al. [1,2]. In this previous work, the crack configuration prior to crack growth was modelled using one nodal point as the crack tip, and the steps of growth were many times larger than any intensely strained region that would arise if the original crack were allowed to have a blunt tip. The results obtained here are for growth step sizes about the same size as the region affected by the blunting of the original crack tip. Differences between the results here and those of Kfouri et al. [1,2] seem most easily explained in terms of the differences in stress prior to crack growth in the regions in which the crack growth occurred.

ACKNOWLEDGEMENT

The author is indebted to Professor J. R. Rice for helpful discussions of this topic. The author received support from the U. S. Energy Research and Development Administration under contract E(11-1)3084 to carry out this work.

References

[1] Kfouri, A. P., and Miller, K. J.,"Crack separation energy rates in elastic-plastic fracture mechanics,"submitted to Proc. Inst. Mech. Eng. (London) 1976.

[2] Kfouri, A. P., and Rice, J. R.,"Elastic/plastic separation energy rate for crack advance in finite growth steps,"in Fracture, 1977, Proceedings of Fourth International Conference on Fracture, ed. D. M. R. Taplin et al., Solid Mechanics Division Publication, University of Waterloo, Canada, Vol. 1, also Technical Report MRL E-98, Division of Engineering, Brown University, Providence, June 1976.

[3] Rice, J. R., Proceedings of First International Conference on Fracture, T. Yokobori et al., Jap. Soc. Strength and Fracture of Materials, Tokyo, 1, 1966, 309.

[4] Schijve, J., in Advances in Aeronautical Sciences, Pergamon Press, London, Vol. 3, 1972, 387.

[5] Paris, P. C., Private Communication, 1975.

[6] Rice, J. R., in Fracture: An Advanced Treatise, ed. H. Liebowitz, Academic Press, New York, Vol. 2, 1968, 191-311.

[7] McMeeking, R. M., "Finite Deformation Analysis of Crack Tip Opening in Elastic-Plastic Materials and Implications for Fracture Initiation," Technical Report E(11-1)3084/44, Division of Engineering, Brown University, Providence, May 1976, also see Ph.D. Dissertation, Brown University, 1976.

[8] Hertzberg, R. W., in Fatigue Crack Propagation, S.T.P. 415, American Society for Testing and Materials, Philadelphia, Pa. 1967, 205.

$\Delta a/(K/\sigma_o)^2$	$\Delta a/(J_{app}/\sigma_o)$	$\Delta a/b$	$W_t/\Delta a$	$W/\Delta a$
3.31×10^{-4}	.109	.230	2.48×10^{-2}	2.48×10^{-2}
1.62×10^{-3}	.535	1.13	4.30×10^{-2}	5.16×10^{-2}
3.94×10^{-3}	1.30	2.74	3.74×10^{-2}	5.21×10^{-2}
6.10×10^{-3}	2.01	4.23	3.17×10^{-2}	4.47×10^{-2}
1.24×10^{-2}	4.10	8.64	2.20×10^{-3}	3.58×10^{-2}

TABLE Showing size of initial step of finite crack growth, Δa, in units of $(K/\sigma_o)^2$, J/σ_o and the width, b, prior to crack growth of the monotonically loaded, blunted notch. Also shown is the distance between the surfaces created by the growth step at the tip of the monotonically loaded, blunted notch (W_t) and at the widest point between the surfaces (W).

List of Figure Captions

Figure 1. Plot of stress $\sigma_{\theta\theta}/\sigma_o$ and plastic strain around the monotonically loaded blunted crack tip for $\sigma_o/E = 1/300$ and $N = 0.1$. Note σ_o is the yield stress in tension and R and θ are defined for the position of the material in the undeformed configuration.

Figure 2. Typical shape of crack tip after a complete finite growth step.

Figure 3. Separation energy rates for initial step of finite growth for various amounts of crack growth.

Figure 4. Dependence of χ on S for initial step of finite growth.

Figure 5. Stress ahead of the crack tip, both prior to and subsequent to the initial step of crack growth.

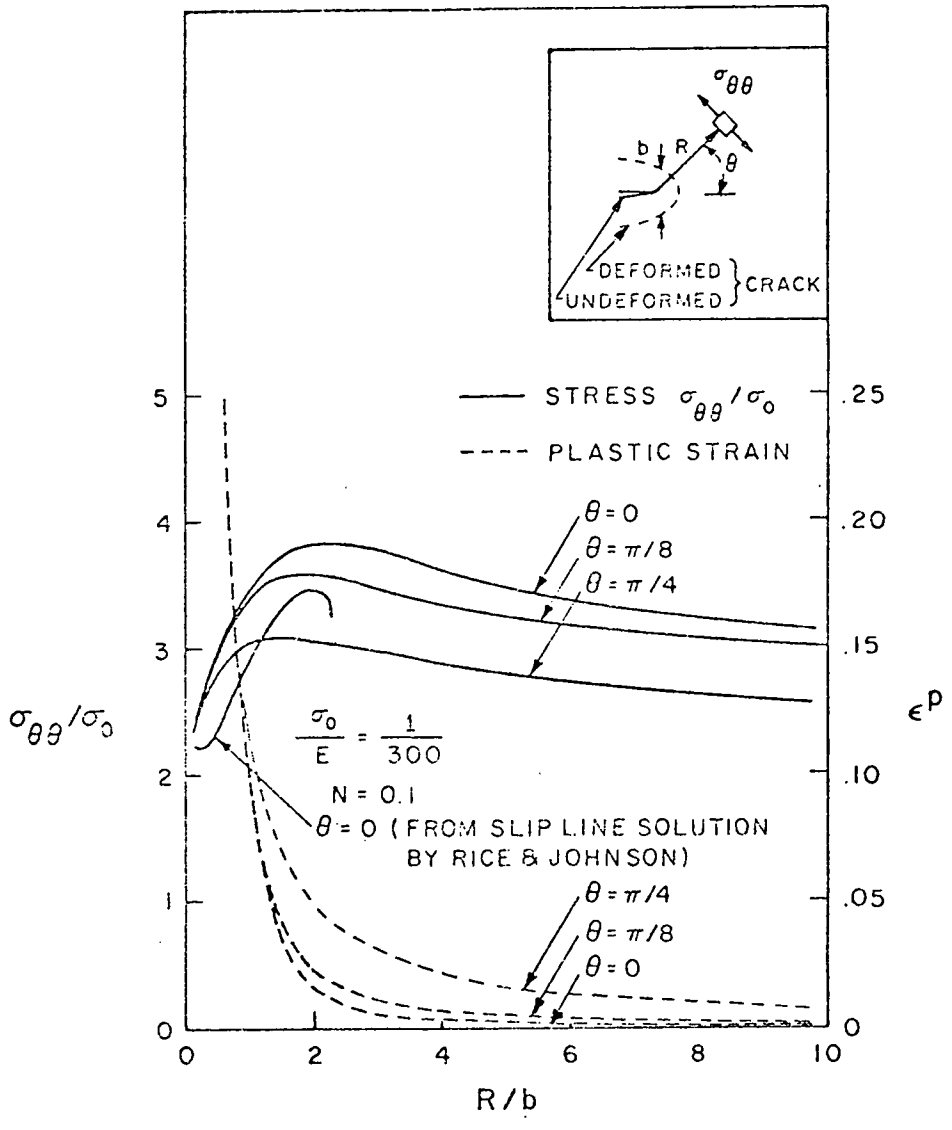
$\sigma_{\theta\theta}$
b
R
θ
DEFORMED
UNDEFORMED
CRACK
STRESS $\sigma_{\theta\theta}/\sigma_0$
PLASTIC STRAIN
$\theta = 0$
$\theta = \pi/8$
$\theta = \pi/4$
$\frac{\sigma_0}{E} = \frac{1}{300}$
N = 0.1
$\theta = 0$ (FROM SLIP LINE SOLUTION BY RICE & JOHNSON)
$\theta = \pi/4$
$\theta = \pi/8$
$\theta = 0$
$\sigma_{\theta\theta}/\sigma_0$
ϵ^p
R/b
0
1
2
3
4
5
.05
.10
.15
.20
.25
0
2
4
6
8
10

Figure 1

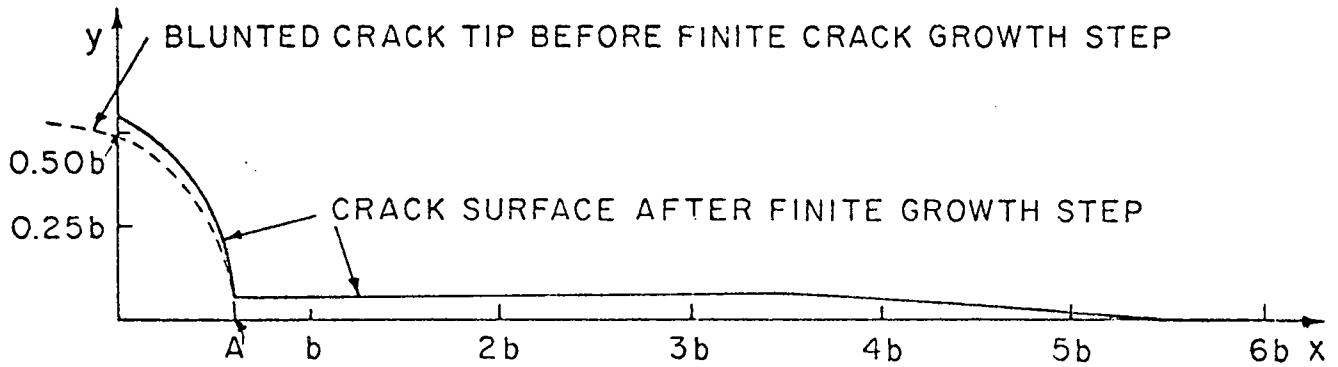

NOTE: CRACK SURFACES ARE DRAWN SO THAT POINT A IS DISPLACED VERTICALLY ONLY.

Figure 2

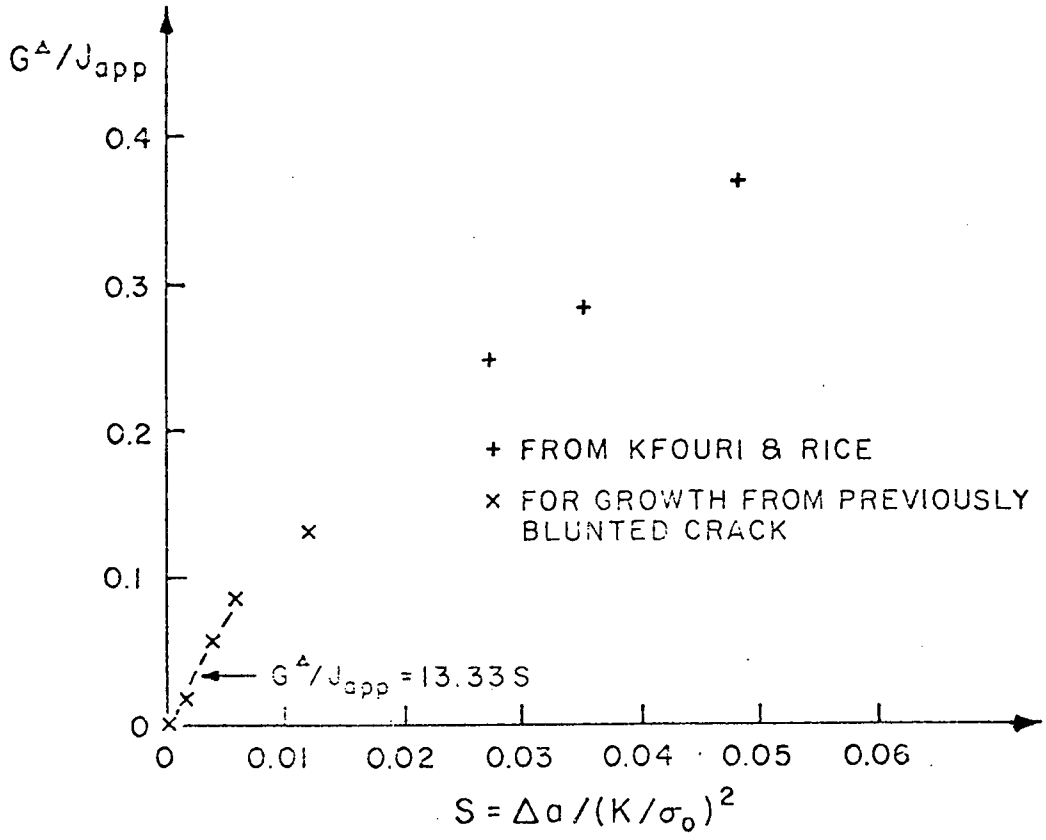
G^{Δ}/J_{app}
0.4
0.3
0.2
0.1
0
+ FROM KFOURI & RICE
× FOR GROWTH FROM PREVIOUSLY BLUNTED CRACK
$G^{\Delta}/J_{app} = 13.33\,S$
0
0.01
0.02
0.03
0.04
0.05
0.06
$S = \Delta a/(K/\sigma_0)^2$

Figure 3

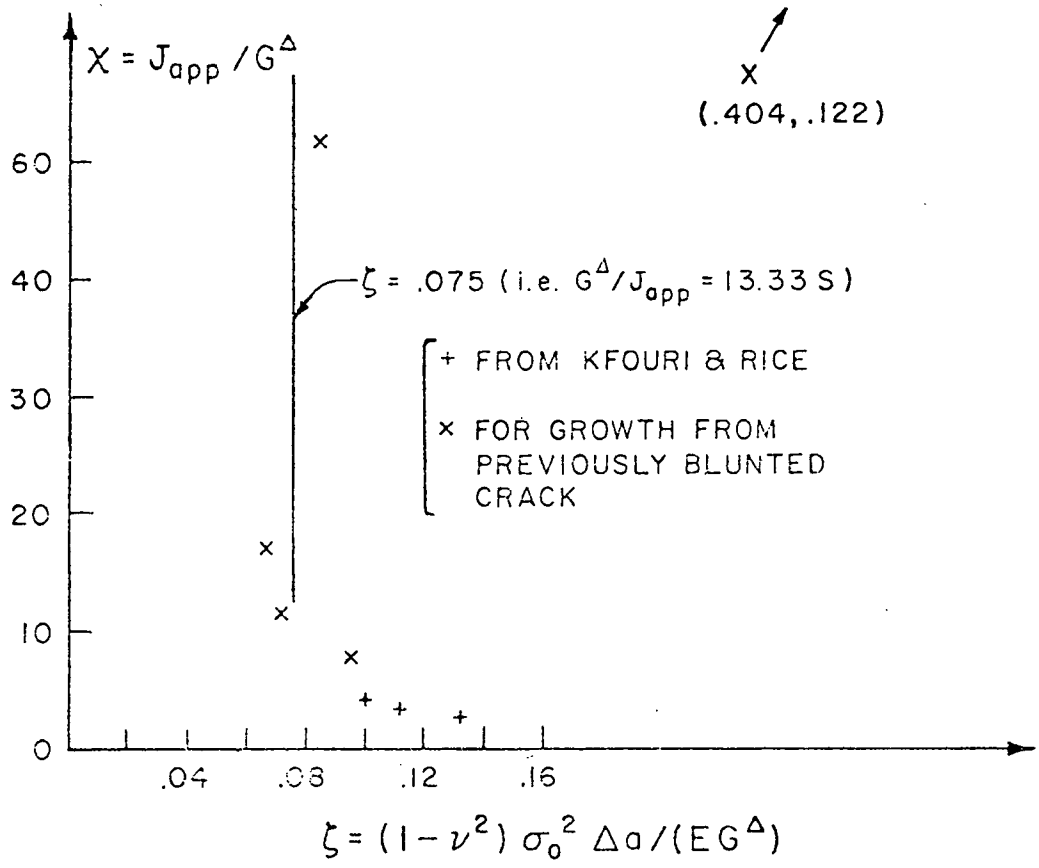
$\chi = J_{app}/G^{\Delta}$
(.404, .122)
60
40
30
20
10
0
ζ = .075 (i.e. G^{Δ}/J_{app} = 13.33 S)
+ FROM KFOURI & RICE
× FOR GROWTH FROM PREVIOUSLY BLUNTED CRACK
.04
.08
.12
.16
$\zeta = (1-\nu^2)\,\sigma_0^2\,\Delta a/(EG^{\Delta})$

Figure 4

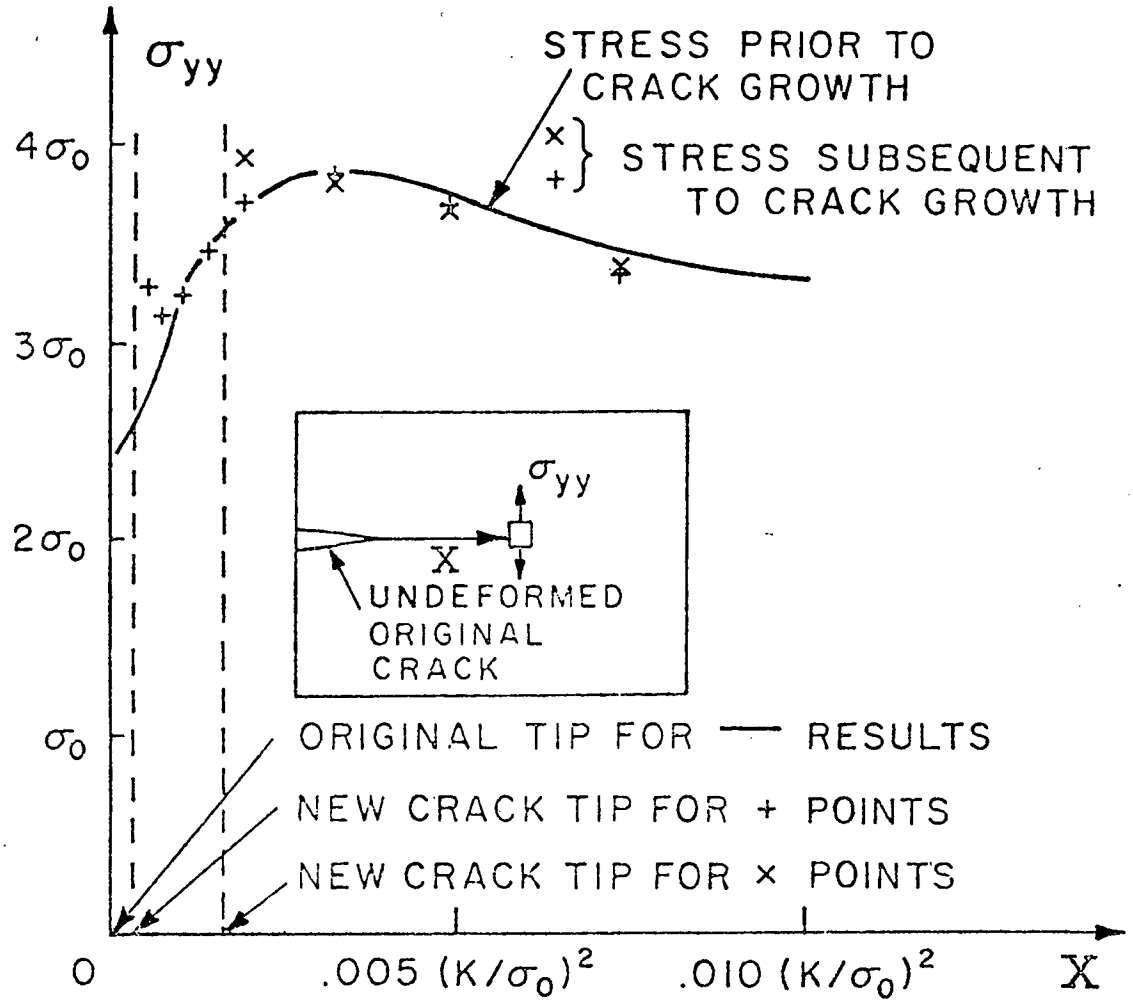
σ_{yy}
STRESS PRIOR TO CRACK GROWTH
STRESS SUBSEQUENT TO CRACK GROWTH
$4\sigma_0$
$3\sigma_0$
$2\sigma_0$
σ_0
σ_{yy}
X
UNDEFORMED ORIGINAL CRACK
ORIGINAL TIP FOR — RESULTS
NEW CRACK TIP FOR + POINTS
NEW CRACK TIP FOR × POINTS
0
.005 $(K/\sigma_0)^2$
.010 $(K/\sigma_0)^2$
X

Figure 5

IV. BLUNTING OF A PLANE STRAIN CRACK TIP INTO A SHAPE WITH VERTICES*

Summary When monotonically increasing tensile opening loads are applied to a cracked, plane strain, elastic-plastic body, the crack tip will blunt until fracture occurs. At least within the rigid-plastic model for non-hardening material, the shape of the blunted tip is not unique. The blunted tip shape may have two or more sharp corners, or be smoothly curved. When the shape involves corners, the opening is predominantly accommodated by shearing of the material at the corners. This shearing transports material from the interior of the body onto the crack surface. In contrast, the smoothly blunted crack tip involves no such transfer of material points from the interior. However, the smoothly blunted crack, which was originally sharp, involves infinite strains on the crack tip surface. The crack with corners on the tip has large but finite strains on the crack tip surface.

The stress and deformation field in front of a crack with two corners and with three corners on the tip, as calculated using the slip line method, is presented for the non-hardening, fully plastic, deeply cracked, double edge-notched thick panel. As in the case of the smoothly blunted crack tip [1], the elevated stress between the crack tips cannot be maintained very close to the crack tip, due to a lack of constraint. The stress distribution in the case of the crack tip with vertices on it differs from that of the smoothly blunted crack tip case. In particular, immediately in front of the crack tip with three corners, the stress is higher than that immediately in front of the smoothly blunted crack tip. An approximation for a power law hardening material indicates that the

maximum stresses near the blunted crack tip is much the same for a crack with vertices on the tip as for a smoothly blunted crack tip. The details of the stress distribution, though, will depend on the mechanism by which the crack blunts. These results for stress and strain and some calculations of the growth of voids near the crack tips indicate the same fracture process could lead to different fracture toughnesses, depending on the type of mechanism by which the crack blunts.

---

* This is a chapter of the author's Ph.D. thesis, Brown University, June 1977.

INTRODUCTION

Many ductile fracture processes are known to take place within a region near the crack tip that is intensely strained or sheared as the crack tip blunts open [1]. It would thus seem to be important to work out the details of the near tip stress and strain fields around the crack tips that are opened up by tensile loads. McClintock [4] has given slip line fields that arise around crack tips that blunt by localized shearing at corners on the crack tip. The corners on the crack tip are connected by straight segments of crack tip surface and McClintock has worked out slip fine fields for crack tips with two and with three corners on the crack tip. McClintock [4] has observed the opening of a macroscopic notch by a mechanism of shearing at two corners, while Clayton and Knott [5] have observed localized shearing at many corners on a macroscopic notch tip. Although the observations were made on notches, the examples are considered to be relevant to blunting crack tips. On the other hand, Rice and Johnson [1] have suggested that the blunting can take place by a general stretching of material on the crack tip. They also worked out the details of the stress and deformation near these smoothly blunted crack tips by using the slip line method. Their results were for the case of small scale yielding, and for the fully plastic deeply cracked double edge-notched specimen. Their results, at least for the case of small scale yielding, have been confirmed by McMeeking [11], who investigated the smooth blunting of the crack tip in an elastic-plastic material using the finite element method. Rawal and Gurland [12] have observed the smooth mechanism of blunting in the opening of a pre-fatigued crack in spheroidized steel. The type of blunting which arises in a specific case may depend on considerations

of strain hardening and stability [4]. The tendency for deformation to localize at, say, asperities on the tip surface may be important in this respect [4].

Apart from the shape, the main difference between the smoothly blunted crack tip case and the case with sharp corners is that the sharp corners are the focus of fans with singular shear strain rates. It is these that largely accommodate the crack opening by transporting material from the interior to create new surface. The result is a strain of order unity on and near the crack tip surface. In contrast, near a smoothly blunted crack tip, an area can be found in which the average plastic strain greatly exceeds unity. Since achieving a critical plastic strain over a critical finite area is a candidate fracture criterion, there could be some significant differences between smooth and vertex blunting of crack tips as far as fracture behavior is concerned. A similar situation arises for stress. In small scale yielding or in the fully plastic yielding of a double edge-notched, deeply cracked panel, the triaxiality in front of the crack tip cannot be maintained near the crack tip when any kind of blunting occurs. However, the distance over which the mean normal stress falls from its elevated level to the lower level near the crack tip depends on the kind of blunting that occurs. Taking as a candidate fracture criterion the achievement of a critical stress over a critical area, one sees that significant differences between the blunting mechanisms are possible as far as fracture is concerned. This carries over to a fracture mechanism involving voids near the crack tip, since void growth is dependent on plastic strain and hydrostatic stress [2,3] and the rate of void growth relative to the rate of crack opening will be influenced by the type of blunting which is occurring.

NON SMOOTH BLUNTING OF CRACK TIPS

The method, by which the details of the near tip field for a blunted crack with vertices on the tip are obtained, is the approach used by Rice and Johnson [1]. They viewed near tip rigid-plastic slip line solutions as good approximations to the behavior of elastic-plastic materials, when elastic strains are neglected compared to plastic strains. They concentrated on the cases of the contained yielding of a plane strain, non-hardening specimen (CY specimen), and the fully plastic yielding of a deeply cracked, double edge notched, thick panel of non-hardening material (DEN panel). One approach to both these problems is to view the crack tip as a point of singular shear strain, and the slip line field of Fig. 1 arises in this case. In the DEN panel, Fig. 1 is the near tip region of the Prandtl punch type plastic zone that arises for full scale yielding [6]. The CY specimen has the slip line field of Fig. 1 only in a near tip region that is small compared to the plastic zone as discussed by Rice [7]. A straight slip line in region C transmits a constant velocity parallel to itself. This velocity was deduced to be approximately

$$v_r = \dot{\delta}_t[\cos(\phi-\pi/4) - \cos 2(\phi-\pi/4)]/(2\sqrt{2}) \qquad (1)$$

for the CY specimen by Rice [7], guided by some etching studies. This seems to be approximately consistent with Rice and Tracey's [13] elastic-plastic finite element results. These indicate that the singular shear strain rate in the fan has a strength which, when expressed as a function of ϕ, is symmetric about $\phi = \pi/2$ and nearly vanishes at the limits of the fan. On the other hand, when there are no discontinuities of velocity on the slip lines between A and C, and between C and B in the

DEN panel, the velocity on the slip lines in C is

$$v_r = \dot{\delta}_t[\sin(\phi-\pi/4)]/(2\sqrt{2}) \ , \qquad (2)$$

as noted by Rice and Johnson [1].

Rice and Johnson [1] noted that when the crack blunts, the fans of singular shearing above and below the crack tip would become non-centered above and below a region of intense stretching adjacent to the blunted crack tip as in Fig. 2. When viewed on the size scale of the plastic zone, this whole region of intense stretching still appears as a point, so the velocities (1) and (2) still serve as approximations to the normal velocities on the outer slip lines of the intensely stretched zone. Note that (1) and (2) were chosen so that the point $(\alpha = 0 \ , \ \beta = 0)$ is stationary. Consequently, Rice and Johnson used these velocities as boundary conditions to solve the slip line equations (Hill [8], pp. 128-140) for the velocity in D.

These equations are

$$\partial v_\alpha/\partial\alpha - v_\beta = \partial v_\beta/\partial\beta + v_\alpha = 0 \ , \qquad (3)$$

where v_α is the component of velocity parallel to lines of constant β and v_β is the component of velocity parallel to lines of constant α. The solution for $v_\alpha(\alpha,\beta)$, $v_\beta(\alpha,\beta)$ was obtained by finite difference integration along the characteristics or slip lines α = constant and β = constant. Note that the position of (α,β) in the physical (x,y) plane was then unknown. However, Rice and Johnson [1] showed that the position of the crack tip, relative to the point $\alpha = 0 \ , \ \beta = 0$, can

be worked out once the velocities on the crack tip are known, as long as the velocities on the tip of the blunted crack remained constant, as in the CY specimen and DEN panel. Once the tip shape was established, the equations

$$\frac{\partial y/\partial \alpha}{\partial x/\partial \alpha} = - \frac{\partial x/\partial \beta}{\partial y/\partial \beta} = \tan (\alpha+\beta+\pi/4) \qquad (4)$$

were integrated by finite difference method along the characteristics to establish the position of the slip line intersection (α,β) in the physical plane. The result is shown in fig. 3. Note the similarity in the results for the CY specimen and the DEN panel.

The crack tip shapes and slip lines for the case of blunting with two corners on the tip and with three corners on the tip are shown in figs. 4 and 5. These figures show the situation for the DEN panel, which should presumably be similar to the CY results. The DEN case was worked out because the included angles of the fans of slip lines can be simply deduced, following McClintock [4]. To obtain the shapes in figs. 4 and 5, some of the results for velocity obtained by Rice and Johnson can be utilized directly. The velocities that can be used are the v_α and v_β components for points lying in the hatched region of the characteristic α,β plane in figs. 4 and 5. The normal velocities on the boundaries of the hatched regions provide boundary conditions for the adjacent regions in the physical (x,y) plane. These adjacent regions contain one family of straight slip lines normal to the boundaries between the region with the straight slip lines and the region hatched in the characteristic plane. A straight slip line carries a constant velocity component, v_p, parallel to itself.

The positive sense of v_p in the regions containing one family of straight slip lines is defined so that positive v_p is directed away from the focus or involute of the straight slip lines. The component of velocity normal to the straight slip lines is v_t, with a positive sense that is $\pi/2$ radians from the positive sense of v_p. The governing equation for velocities in the regions with one family of straight slip lines is

$$dv_t(\theta)/ d\theta + v_p(\theta) = 0 \quad , \qquad (5)$$

where θ is the angle the straight slip line makes with the x-axis. The equation (5) may be integrated subject to a boundary condition of known v_t on one side of the region with one family of straight slip lines. In the flat nosed case, fig. 4, and in the case of the regions with one family of straight slip lines not attached to G in fig. 5, the boundary condition for integrating (5) is the appropriate value of v_r taken from (2). The boundary condition for the fans attached to G in fig. 5 comes from the results of the integration of (5) for the non-centered fan between regions I and II. The remaining regions, with two families of straight slip lines, are non-deforming.

That the deduction concerning the included angles of the fans of slip lines in figs. 4 and 5 was correct may be checked by noting that there are no velocity discontinuities at any of the slip lines in regions A, B and C of fig. 1. Thus, there will be no velocity discontinuities on any slip lines in the regions near the crack tip with corners, equivalent to region D in fig. 2. Since the velocities are calculated by two different methods on either side of the slip lines separating the regions with one family of straight slip lines

from the regions hatched in the characteristic plane, agreement between the velocities computed on either side of these slip lines means that the deduction was correct.

The net results obtained are the constant velocities of each straight surface segment on the crack tip. The component of this velocity normal to the straight surface segment, say $V_n \overset{e}{\delta}_t$, may be integrated in time to give the position of the straight surface segment. The position, measured relative to axes attached to the point with $\alpha = 0$, $\beta = 0$, is such that the length of the normal from the segment to the original position of the crack tip is $V_n \delta_t$. Now that the position of the crack tip is known, the configuration of the slip lines in front of the crack can be worked out. In regions in which there is at least one family of straight slip lines, consider any two straight segments of slip line running between the same two members of the other family of slip lines. According to Hill ([8], p. 138), these straight segments have equal length. In particular, this means that the centered fans of slip lines in figs. 4 and 5 are segments of a circle, and the radius can be calculated from the geometry of the crack tip. This establishes the shape of two intersecting sides of the region containing two families of curved slip lines, not touching the x-axis. These shapes may be used as boundary conditions for the finite difference integration of (4) along the characteristics. Now the shape of one curved side of the region containing one family of non-focused straight slip lines is known, as well as the length of one of the straight sides of this region. This serves to establish the shape of two intersecting sides of the remaining region of curved slip lines,

and (4) may be integrated once more to complete the shape of the near tip slip lines. In this way, the exact shapes of figs. 4 and 5 were established.

STRAIN AHEAD OF THE CRACK TIP

The strain on the x-axis ahead of the tip of the cracks of Figs. 4 and 5 may be computed from the numerically known velocity and position of material points. Following Rice and Johnson [1], the parameter ψ is introduced for representing the velocity and position on the x-axis in the regions with two families of curved slip lines. This parameter is defined as

$$\psi = \pi/2 - 2\beta \quad \text{on} \quad \alpha + \beta = 0 \quad . \tag{6}$$

The x-axis is, of course, the line $\alpha + \beta = 0$. Note that $\psi = \pi/2$ at the point A, figs. 4 and 5, in both the flat nosed and the sharply tipped case. In the flat nosed case, $\psi = 0$ at D and in the sharply tipped case, $\psi = \pi/6$ at F . The velocity in the x-direction on the x-axis in the regions of interest may be written

$$v_x(x,0) = \dot{\delta}_t V(\psi) \quad , \tag{7}$$

and similarly the position of the point represented by ψ is known numerically in the form

$$x = \delta_t F(\psi) \quad . \tag{8}$$

Following [1], eq. (8) may be differentiated with respect to time and equated to (7) to give

$$F(\psi) + \delta_t F'(\psi)\partial\psi(X,\delta_t)/\partial\delta_t = V(\psi) \quad , \tag{9}$$

where X is the position of a material point before any deformation. This equation may be integrated by noting that the crack tip opening at the time when a point A reaches X is $X/F(\pi/2)$; that is, when the small deformations

occurring to the right of point A are neglected. The result of the integration is [1]

$$X = \delta_t H(\psi) \quad \text{where} \quad H(\psi) = F\left(\frac{\pi}{2}\right) \exp\left\{ -\int_{\psi}^{\pi/2} \frac{F'(\psi)d\psi}{F(\psi)-V(\psi)} \right\} . \qquad (10)$$

The deformation gradient is thus

$$\partial x(X,\delta_t)/\partial X = \delta_t F'(\psi)\partial\psi(X,\delta_t)/\partial X = F'(\psi)/H'(\psi) \quad . \qquad (11)$$

Defining the true strain ε_x^{tr} as $\log(\partial x/\partial X)$ and noting that $\varepsilon_y^{tr} + \varepsilon_x^{tr} = 0$, it can be seen that

$$\varepsilon_y^{tr} = \log \frac{H'(\psi)}{F'(\psi)} = -\int_{\psi}^{\pi/2} \frac{V'(\psi)d\psi}{F(\psi)-V(\psi)} \quad . \qquad (12)$$

This derivation illustrates the manner in which the strain at a material point is accumulated as the near tip slip line field expands, and causes the material point to move, figuratively, from point A towards point D in Fig. 4, and from point A towards point F in Fig. 5. Once the material point enters the region between D and E or between G and F, the deformation ceases and the strain is constant in these regions.

The true strain calculated from (12) is plotted in Fig. 6 against undeformed position calculated from (10), and the strain in the non-deforming regions is plotted as well. The stretches on the X-axis remain relatively small compared to the larger values near the tip of a smoothly blunted crack. Note, however, that in the region where $1 < X/\delta_t < 2.5$, a slightly more severe strain state is achieved in the cases where the crack has blunted by the sharp corner mechanism. In terms of a fracture process that occurs when a critical strain is achieved over a critical length, the crack tip opening displacement at fracture would be slightly greater in the smoothly

blunted case compared to the sharp nosed case; that is, if the X-axis strain is typical. Note that the material on the X-axis from $X = 0$ to $X = 0.49$ is currently lying on the crack tip surface. The sharp nosed case would show a slightly larger δ_t at fracture compared to the flat nosed case, at least based on crack growth occurring on the x-axis. If the critical true fracture strain is greater than 0.25, there will be no fracture in that particular mode which involves rupture along the X-axis at a sharp nosed crack. Similarly, if the critical true fracture strain is greater than 0.625, no fracture in the associated mode along the X-axis would occur at a flat nosed crack. It would seem to be very likely that in the model for blunting involving shearing at sharp corners there will be strains off the X-axis that are greater than the strains achieved on the X-axis. Since a point currently lying in the non-deforming regions will have experienced different strain histories depending on their positions within the non-deforming region, the strains in the non-deforming regions are not uniform. However, the strains everywhere will be finite, although rising to magnitudes of order unity in the regions adjacent to the crack tip.

In addition to the stretching of material in front of the crack tip, there are shear strains that arise on the crack tip surface. These are due to the fans of singular shearing attached to the crack tip. The total plastic strain due to the shearing may be worked out as follows. Consider a fan with constant orientation and included angle. The fan origin is, however, being transported at a constant velocity, $\underset{\sim}{v}^{o}$, relative to point A. Simultaneously the radius of the fan increases, although this is not immediately relevant.

An origin is attached to the focus of the fan, and polar co-ordinates (r,θ) are defined relative to this origin. The quantity of interest is the plastic strain accumulated at a material point which is first enveloped by the fan at co-ordinates (r_o,θ_o), where r_o is less than the outer radius of the fan. Attention will be restricted to the situation where the fan lies in the area where $\theta > \theta_o$. This restriction is trivial, since the fan lying either above or below the x-axis may be chosen to meet this condition. In the fan, the velocity of points is known numerically in terms of the polar components, v_r^f, v_θ^f. These velocities are relative to point A, and depend only on the current value of θ at the point of interest. Thus, the velocity of the point currently at (r,θ) in the fan is $\underset{\sim}{v}^r(\theta) = \underset{\sim}{v}^f(\theta) - \underset{\sim}{v}^o$ relative to the moving focus of the fan. In particular, the relative angular velocity is

$$\dot{\theta} = (v_\theta^f(\theta) - v_\theta^o)/r \qquad (13)$$

The rate of change of plastic strain $\dot{\varepsilon}_p = \sqrt{2D_{ij}^p D_{ij}^p/3}$, $2D_{ij} = (\partial v_i/\partial x_j + \partial v_j/\partial x_i)$ is

$$\dot{\varepsilon}_p(\theta) = [\partial v_r^f(\theta)/\partial\theta - v_\theta^f(\theta)]/(r\sqrt{3}) \quad . \qquad (14)$$

Equation (14) may be divided by (13) and the result integrated from θ_o to θ_f, where θ_f is the angular co-ordinate when the point leaves the fan. This gives the total plastic strain accumulated in the fan by the material point. The result is

$$\varepsilon_p(\theta_f) - \varepsilon_p(\theta_o) = \int_{\theta_o}^{\theta_f} \frac{[dv_r^f(\theta)/d\theta - v_\theta^f(\theta)]d\theta}{\sqrt{3[v_\theta^f(\theta) - v_\theta^o]}} \quad . \qquad (15)$$

This quantity is independent of the radius, r_o , at which the material point enters the fan. Therefore, it is the plastic strain accumulated by any material point that passes through the fan, including material that passes through the tip of the fan. The point that passes through the tip is deposited on the crack tip surface.

The integral (15) was calculated numerically for material passing through the tip of the fan attached to corner C in fig. 4, and for material passing through the tip of the upper fan attached to point G in fig. 5. In the flat nosed case, the material passing though the tip of the fan accumulates a plastic strain of 1.003. This material passes from a non-deforming region above and below the crack tip into the tip of the fan at C. In general, it will have accumulated some plastic strain while it lay in the non-centered fan of slip lines above and below the crack tip, that is, before it entered the non-deforming region. However, the points on the crack surface just above and below E will have experienced negligible deformation before passing through the fan attached to C. Thus, around point E, on the crack surface, there is a plastic strain of 1.00. In the sharp nosed case, the material that passes through the tip of the fan attached to G picks up a plastic strain of .760 while in the fan. This material has already been stretched to a plastic strain of .278, so that plastic strain of points on the crack surface adjacent to the point G is 1.04. These strains have been plotted in the appropriate manner in fig. 6.

STRESSES AHEAD OF A BLUNTED CRACK

As noted by Rice and Johnson [1], the mean normal stress ahead of the crack tip is

$$\sigma = [1+\pi+2(\alpha-\beta)]\sigma_o/\sqrt{3} \qquad (16)$$

in the regions containing two families of curved slip lines. The term σ_o is the yield stress in uniaxial tension. On the x-axis, there is also a purely deviatoric stress of $\sigma_y' = \sigma_o/\sqrt{3}$, $\sigma_x' = -\sigma_o/\sqrt{3}$. The total stress, $\sigma_y/\sigma_o = (\sigma_y' + \sigma)/\sigma_o$, has been plotted as the full line in Figs. 7, 8 and 9,for the smoothly blunted crack tip, the blunted crack tip with two corners,and with three corners respectively. In the last two cases, use has been made of the fact that the regions with two families of straight slip lines are regions of constant stress state, the stress state being the same as that for the immediately adjacent regions. It can be seen that the stress state in the region further from the crack tip than $X = 2.6\delta_t$ is the same for all three cases. In the two cases where the crack tip cuts the x-axis at 90°, the stress, σ_y , is the same on the crack surface with a value equal to the yield stress in plane strain tension. Where a corner on the crack tip lies on the x-axis, the stress σ_y on the x-axis at the crack tip is elevated above the plane strain tensile yield stress.

Following Rice and Johnson [1], an approximation to the stress for power law-hardening materials was obtained. Essentially, the technique is to assume that the plastic strain distribution is accurate ahead of the crack tip. This assumption is quite appropriate, according to the results of McMeeking [11]. The flow stress, and consequently the deviatoric

stress, can be calculated from the plastic strain according to the power law relationship assumed. Then the equilibrium equation,

$$\partial\sigma_{xx}/\partial x + \partial\sigma_{xy}/\partial y = 0 \quad , \tag{17}$$

can be integrated along the x-axis to provide the hydrostatic part of the stress. The term $\partial\sigma_{xy}/\partial y$ is evaluated from the curvature of the slip lines as they cross the x-axis, and the necessary boundary condition is provided at the traction free surface of the crack. However, on the free surface on the X-axis, there is a vanishingly thin layer of elevated plastic strain in the cases of blunting with corners on the tip. Furthermore, in the case with three corners on the tip, there is the complication of the singular shearing at the corner on the x-axis. If one assumes that the region between D and E in fig. 4 is still one in which $\sigma_{xx} = 0$, then σ_{yy} may be calculated there as 1.15 times the uniaxial tensile flow stress at a plastic strain of .727, which is the plastic strain for points lying between D and E. Similarly, using the stress levels between G and F in the non-hardening material as a guide, the boundary condition chosen for G in fig. 5 to integrate (5) for a hardening material was that σ_{yy} should be 1.76 times the uniaxial tensile flow stress calculated for the plastic strain at points between G and F. These boundary conditions are essentially those that would be obtained in the absence of elevated plastic strain on the tip surface.

The power law relationship that was used in the integration of (17) was

$$\bar{\sigma} = \sigma_o(\bar{\varepsilon}^p E/\sigma_o+1)^N \quad , \tag{18}$$

where $\bar{\sigma}(= \sqrt{3}\ (\sigma_{yy}-\sigma_{xx})/2$ on the x-axis) is the uniaxial tensile flow stress, $\bar{\varepsilon}^p(=2\varepsilon_y^{tr}/\sqrt{3}$ on the x-axis) is the total plastic true strain in

uniaxial tension and E is Young's modulus. This law differs in form from that of Rice and Johnson [1], who used

$$\bar{\sigma} = \sigma_o(\bar{\varepsilon}E/\sigma_o)^N \quad , \tag{19}$$

where $\bar{\varepsilon}$ is the true strain in uniaxial tension. They set $\bar{\varepsilon} = 2\varepsilon_y^{tr}/\sqrt{3}$ on the x-axis. The difference is simply one of interpretation. Rice and Johnson regarded the strain on the x-axis as an approximation to the total strain there (elastic plus plastic strain). The difference between total strain and plastic strain only becomes significant near point A, where the elastic strains, if they were calculated, would be similar in magnitude to the plastic strains. Since $\varepsilon_y^{tr} = 0$ at A, as in Fig. 6, the approximation that Rice and Johnson used is really for a continuously hardening material with zero yield stress, and no allowance was made for elastic strains around point A. However, if (18) is used, the flow stress at point A is the yield stress in uniaxial tension, with the idea that strains of order σ_o/E are present to the right of point A in fig. 3. At the point A, and for some distance to the left of point A, Rice and Johnson regarded the singular, small strain results of Hutchinson [9], and Rice and Rosengren [10] for the stress near the crack tip in a power law hardening material to be more accurate. In addition, the discrepancy in σ_y between using (18) and using (19) amounts to greater than 2% within a distance of $0.2\delta_t$ from point A. As a result, it is not really of much significance whether (18) or (19) is used to obtain results for the CY specimen. However, at point A, the discrepancy is of the same size as the stress itself. To apply the Hutchinson, Rice and Rosengren result to the near tip region of the fully plastic DEN panel and relate it to the work here, one needs some information concerning the relationship between δ_t

and J/σ_o for the hardening materials, where J is the J-integral of Rice [7]. In the absence of this information, and short of a complete solution, the approximation obtained by integrating (17) subject to (18) is probably the most accurate way of obtaining the stress state around point A in the elastic-plastic DEN panel in the fully plastic condition. At least, this result is the most accurate approximation for the rigid-plastic DEN panel made of a power law hardening material with a finite, rather than zero, yield stress.

The results of this approximation are shown as the broken lines in figs. 7, 8 and 9, where the effect of both hardening exponent and initial yield stress on the stress level can be seen. In the smoothly blunted case, the stress rises to a higher level in the fully plastic DEN panel then in the CY specimen [1]. Thus, if the results are adjusted down to account for this difference in the CY specimen, the stresses for blunting with corners on the crack tip in the CY specimen would seem to be slightly smaller than those in the smoothly blunted crack in the CY specimen. The differences in magnitude would not seem to be significant in view of the approximations involved. The rise and fall of stress occurs over a shorter distance, when measured in terms of crack tip opening displacements. In terms of a fracture event controlled by a critical stress that must apply over a critical distance, specimens with smoothly blunted crack tips would appear to be marginally less tough than those which have cracks blunted by the sharp corner mechanism. Again, the difference would be small enough to compare with the inaccuracies of the analysis. Note, however, that the stress state near the corner on the x-axis of the three cornered crack tip is high compared to the stress state near

the crack tip in the other two cases with different blunting mechanisms. It is possible that this stress, combined with the intense shearing at the corner, provides a destabilizing effect which promotes fracture.

Assuming that the stresses plotted in figs. 7-9 for the power-law hardening materials are reasonable approximations to the correct result for the hardening fully plastic DEN panel, then the net force required to deform the panel may be calculated. Taking the case of $N = 0.1$ and $\sigma_o/E = .0075$, since one might expect that the approximations involved in obtaining the stress plots in figs. 7-9 for this material would be least, one may work out the y-direction net force across the x-axis due to the near tip stress state as plotted in figs. 7-9. It turns out that the force for the crack with the three cornered tip is .92 times the force for the smoothly blunted crack. Similarly, the force for the crack with the two cornered tip is .86 times the force for the smoothly blunted tip. The stress state beyond a distance $2.5\delta_t$ from the crack tip is independent of the type of blunting. To find the net force on the panel, one would sum the force due to the near tip field and the force in the area between the near tip fields. Thus, the difference in the net force on the panel, between a panel with smoothly blunting crack tips and a panel with cracks with corners on the tips, arises entirely from the near tip field. It follows that less force is required to deform the panel with cracks that are blunting by the vertex mechanism, and least is required to deform the crack tip with two on the tip, all compared at the same level of opening, δ_t . Similarly, the rate of work of the loads on the panel would be least if the crack blunts into a shape with the two corners on

the tip, at least within the idealization that the surfaces remote from the crack bound rigid regions. The development suggests the application of the plastic limit theorems (Prager [14]), to predict a most favored deformation, but these theorems can only be applied to specimens which have identical boundary geometries in the deforming region. As a result, no inference can be made about which type of blunting is favored. It should be stressed once more that the inaccuracies involved in obtaining the stresses for hardening materials may be so great as to invalidate the estimates of the difference in net force on the panel. Finally, the stress plots in figs. 7-9 would involve a reduction of the net force on the panel as δ_t is increased, since the near tip field would envelop a continually increasing area. It is to be imagined that the tests are being carried out under displacement control, so that no unstable deformation would occur.

GROWTH OF A VOID NEAR THE CRACK TIP

As discussed by Rice and Johnson [1], a model for ductile fracture involves the growth and coalescence of holes. The same model for void growth will be adopted here as was used by Rice and Johnson [1] and later by McMeeking [11]. This model shows the heavy dependence of void growth on plastic strain and hydrostatic stress, as noted by McClintock [2]. The model was developed by Rice and Tracey [3], and is strictly applicable to an isolated spherical void growing in a remote, uniform stress and deformation field in a rigid-plastic non-hardening material. Rice and Johnson [1] adopted the model, replacing the remote field by the local field of stress and deformation at the current void site in their results for the smooth blunting of a crack. As in Rice and Johnson [1], the equations representing the growth of a hole on the x-axis ahead of the crack tip in the inset of fig. 10 are

$$\begin{aligned} d\bar{a}/\bar{a} &= 0.322 d\varepsilon_y^{tr} \exp(3\sigma/\sigma_o) \quad , \\ da_x/\bar{a} &= -2d\varepsilon_y^{tr} + d\bar{a}/\bar{a} \quad , \\ da_y/\bar{a} &= 2d\varepsilon_y^{tr} + d\bar{a}/\bar{a} \quad , \end{aligned} \tag{20}$$

where a_y and a_x are the major and minor diameters of the ellipsoidal void, and $\bar{a}$ is the mean diameter of the void. In terms of the angle parameter ahead of the crack tip, $\sigma = (1+2\psi)\sigma_o/\sqrt{3}$ and ε_y^{tr} is given by (12) so that

$$\bar{a}(\psi)/a_o = \exp\left\{ 0.322 \int_{\pi/2}^{\psi} \frac{\exp[\sqrt{3}(1+2\psi)/2] V'(\psi)}{F(\psi) - V(\psi)} \, d\psi \right\} \quad , \tag{21}$$

where a_o is the original diameter of the hole. In this, the void is assumed to grow once point A reaches its position. Thus, hole nucleation is assumed to have taken place by the time point A coincides with the position of the

particle from which the void arose. The growth computation can be continued until the void site reaches the crack surface in the case of the smoothly blunting crack tip or until it reaches a non-deforming region in the other cases.

The two principal dimensions of a void growing on the x-axis ahead of the crack tip are shown in Fig. 10 for each of the three types of blunting analyzed. The positive direction along the horizontal scale can be viewed as a relative measure of time. When point A coincides with the spherical void, it begins to grow in each case. The void in front of the flat nosed crack tip grows most strongly at first, while the void in front of the smoothly blunted crack tip grows at a slower rate than the other two voids. As noted, the voids in front of the non-smoothly blunted crack tips cease growing when they enter the non-deforming regions between D and E in Fig. 4 and between G and F in Fig. 5. Thereafter, the size of the void in front of the smoothly blunted crack tip catches up with and overtakes the other void sizes, in terms of the relative time scale δ_t/X_o . As Rice and Johnson have noted, the model for void growth adopted here ignores any influence of neighboring free surfaces. This means that the influence of the crack tip surface on the growth of the void is not accounted for.

In terms of fracture initiation from the existing crack tip, involving voids lying on the X-axis, basically the specimen with the larger holes at a given distance from the crack tip will be least tough [1]. Consequently, if fracture initiation occurs in the range $1 < a_y/a_o < 5.5$, the specimen with the flat nosed crack tip will be less tough in terms of δ_t/X_o than the specimen with the smoothly blunted crack tip, at least based on the behavior of voids on the x-axis.

If the material requires void growth beyond $a_y/a_o = 5.5$ before fracture initiation occurs, then the specimen with the flat nosed crack tip will experience no fracture at all along the X-axis. Similarly, the specimen with a sharp nosed crack tip will experience no fracture initiation along the X-axis, if void growth beyond the level $a_y/a_o = 3.2$ is required to initiate the fracture process. This possible difference in fracture behavior between rupture from smoothly and non-smoothly blunted cracks would appear to be important, because many of the materials which fracture by void growth associated processes, discussed by Rice and Johnson [1] and McMeeking [11], for example, lie in the range of toughness $0.5 < \delta_t/X_o < 1.5$. The different void growth rates could lead to significant differences in predicted toughness, and may help to explain some of the data discussed in [1] and [11]. Of course, knowledge of the predominant mode of blunting in each material would be required.

The validity of the discussion above depends on the behavior of the voids on the x-axis being typical of behavior of voids elsewhere. The situation is likely to be somewhat different for fracture involving voids not lying on the x-axis, since the strains may be somewhat higher for points not lying on the x-axis, at least for cracks that blunt by the sharp corner mechanism. McMeeking [11] has shown that when smooth blunting occurs in small scale yielding, not much difference of growth rate arises between differently positioned voids. In addition, plastic strains everywhere around the crack tip blunted by the corner mechanism are limited. This means that the size of voids around such crack tips is limited, but possibly quite large, compared to undeformed size. The maximum size of voids positioned on the x-axis may be different from the maximum size of voids elsewhere.

CONCLUSIONS

The slip line fields around a crack in a rigid-plastic deeply cracked double edge-notched thick specimen, blunting by the vertex mechanism, is similar to the slip line field around a smoothly blunted crack in the same specimen. In the first case, the crack opening is partly accommodated by singular shearing at the corners on the crack tip, whereas in a smoothly blunted case, the crack opening is accommodated by intense stretching around the crack tip. Intense stretching still occurs where blunting is by the vertex mechanism, but the strain levels are limited, by comparison to the infinite strains that result on the tip of a smoothly blunted crack tip which was originally sharp. The shearing at the corners, however, leaves a plastic strain of order unity on the crack tip surface and in regions nearby.

As in the smoothly blunted case, the triaxial stress induced by the crack cannot be maintained near the surfaces of the tip blunting by the sharp corner mechanism. The stress at the tip is higher on the x-axis in the case of a crack blunting with three corners on the tip than in both the flat nosed case and smoothly blunted case. In both cases of blunting by vertex mechanism studied, there is a constant stress region next to the crack tip on the x-axis. The stress rises from the tip region value to the elevated value away from the crack tip over a shorter distance compared to the distance for the stress to rise to its maximum value when smooth blunting is involved. When an approximation to account for strain hardening is introduced, the maximum stresses away from the tip surfaces when blunting by the vertex mechanism occurs are

close in magnitude to the maximum stresses away from the tip surfaces when smooth blunting is involved.

Void growth rates near crack tips with corners on them are initially larger than the rates of void growth near smoothly blunted crack tips. However, the sizes of the voids near crack tips with corners on them are limited, because plastic strain levels are limited. This means that possibly the specimen with a crack with corners on the tip will have a fracture toughness different from the specimen with a smoothly blunted crack tip. Similarly, differences in fracture behavior due to the type of blunting involved will arise if the fracture process is controlled by either a critical stress or a critical strain that must be applied over a characteristic distance.

ACKNOWLEDGEMENT

The author is indebted to Professor J. R. Rice for helpful discussions of this topic. The author received support from the U. S. Energy Research and Development Administration under contract E(11-1)3084 to carry out this work.

REFERENCES

[1] Rice, J. R., and Johnson, M. A., in Inelastic Behavior of Solids, M. F. Kanninen et al. Ed., McGraw-Hill, New York, 1970, pp. 641-670.

[2] McClintock, F. A., Journal of Applied Mechanics, 25, 1968, p. 363.

[3] Rice, J. R., and Tracey, D. M., Journal of the Mechanics and Physics of Solids, 17, 1969, p. 201.

[4] McClintock, F. A., in Fracture: An Advanced Treatise, M. Liebowitz, Ed., Academic Press, New York, 1971, Vol. 3, p. 47.

[5] Clayton, J. Q., and Knott, J. F., Metal Science, 10, 1976, p.63.

[6] McClintock, F. A., and Irwin, G. R., in Fracture Toughness Testing and Its Applications, STP 381, American Society for Testing and Materials, Philadelphia, 1965, pp. 84-113.

[7] Rice, J. R., Journal of Applied Mechanics, 35, 1968, pp. 379-386.

[8] Hill, R., The Mathematical Theory of Plasticity, Oxford University Press, London, 1950.

[9] Hutchinson, J. W., Journal of the Mechanics and Physics of Solids, 16, 1968, pp. 13-31.

[10] Rice, J. R., and Rosengren, G. F., Journal of the Mechanics and Physics of Solids, 16, 1968, pp. 1-12.

[11] McMeeking, R. M., "Finite deformation analysis of crack tip opening in elastic-plastic materials and implications for fracture initiation," Technical Report E(11-1)3084/44, Division of Engineering, Brown University, Providence, R. I., 1976. Also Ph.D. Dissertation, Brown University, 1976.

[12] Rawal, S. P., and Gurland, J., In Proceedings of the 2nd International Conference on Mechanical Behavior of Materials, Federation of Materials Societies, 1976, p. 1154.

[13] Rice, J. R., and Tracey, D. M., in Numerical and Computer Methods in Structural Mechanics, S. J. Fenves et al. Eds., Academic Press, New York, 1973, p. 585.

[14] Prager, W., An Introduction to Plasticity, Addison-Wesley, Reading, Massachusetts, 1959.

LIST OF FIGURE CAPTIONS

Fig. 1 Near tip stress state and slip line configuration around the crack tip (Rice and Johnson [1]).

Fig. 2 (a) Slip line field around smoothly blunted crack tip,
(b) Map of region D into characteristic plane (Rice and Johnson [1]).

Fig. 3 Deformed shape of crack tip and outer slip line of region D for a smoothly blunted crack tip.

Fig. 4 Deformed shape of crack tip and near tip slip line field when crack blunts by mechanism of two vertices. The slip line from A to B is equivalent to the outer slip line of region D. Also shown is the characteristic plane.

Fig. 5 Deformed shape of crack tip and near tip slip line field when crack blunts by mechanism of three vertices. The slip line from A to B is equivalent to the outer slip line region D. Also shown is the characteristic plane.

Fig. 6 True strain on line ahead of crack, for each type of blunting, as a function of position X of a material point before deformation.

Fig. 7 Solid line shows tensile stress ahead of a smoothly blunted crack tip in a fully plastic non-hardening double edge-notched thick specimen. Non-solid lines are approximate stresses in the same specimen made of a power law hardening material with tensile yield strain σ_o/E and power law exponent N.

Fig. 8 Same as fig. 7, but for a crack tip blunted by the two vertex mechanism.

Fig. 9 Same as fig. 7, but for a crack tip blunted by the three vertex mechanism.

Fig. 10 Plot of dimensions of a void growing near the crack tip on the X axis versus crack tip opening displacement. The crack is in the double edge-notched thick specimen and the results are shown for each type of blunting.

τ_0
$(1+\frac{3\pi}{2}-2\theta)\tau_0$
y
C
A
B
θ
x
$(2+\pi)\tau_0$
$\pi\tau_0$
$2\tau_0$
τ_0
$(1+\pi)\tau_0$

Figure 1

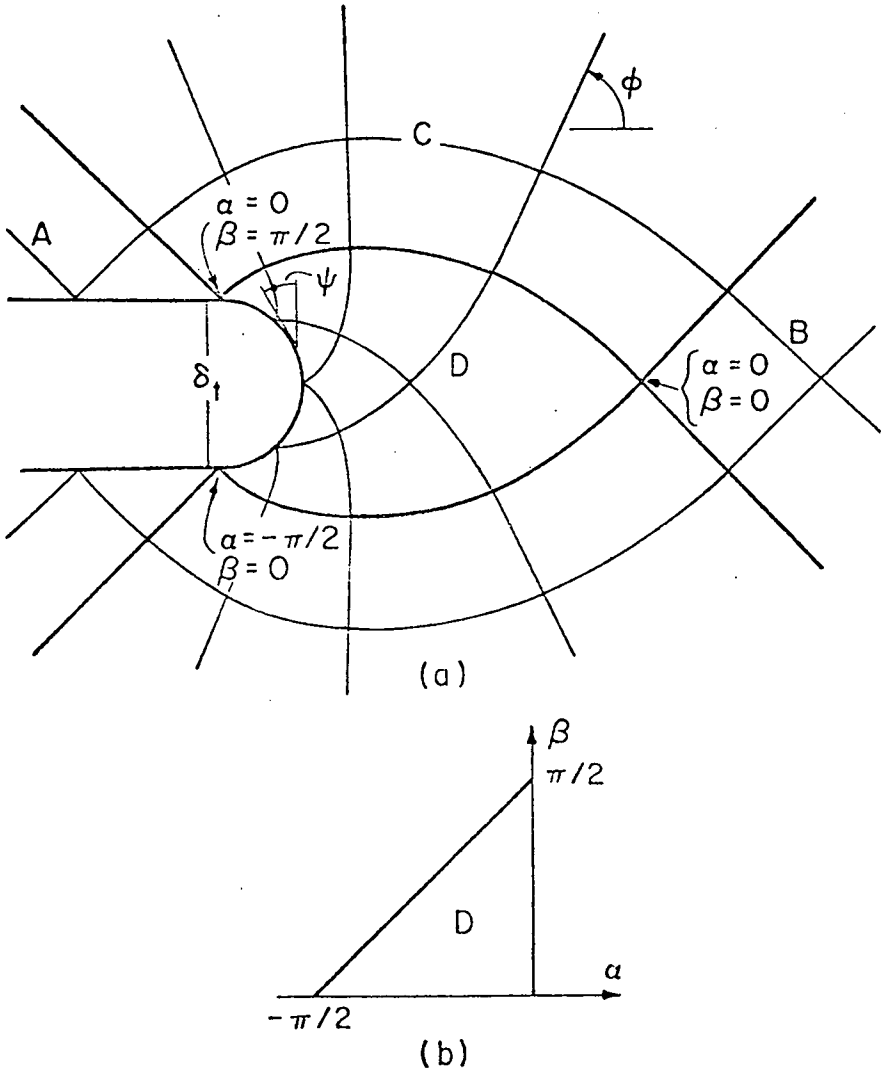

Figure 2

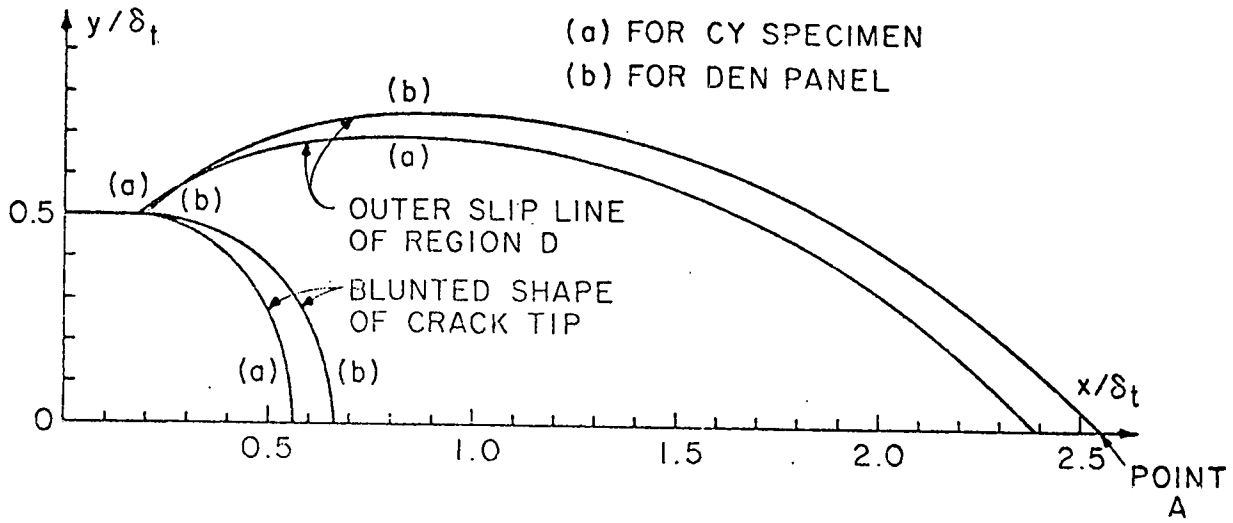
y/δt
(a) FOR CY SPECIMEN
(b) FOR DEN PANEL
(b)
(a)
(a)
(b)
OUTER SLIP LINE
OF REGION D
BLUNTED SHAPE
OF CRACK TIP
(a)
(b)
0.5
0
0.5
1.0
1.5
2.0
2.5
x/δt
POINT
A

Figure 3

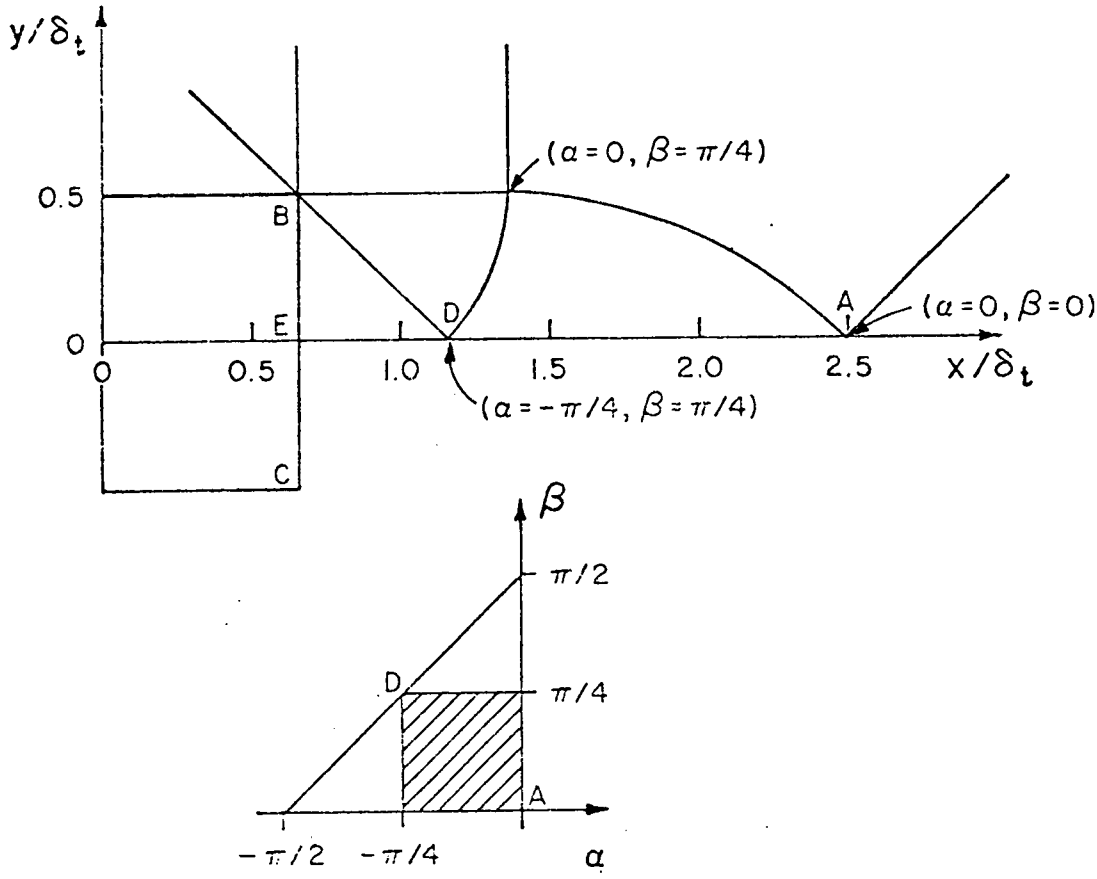
y/δt
0.5
0
B
E
D
A
C
(α = 0, β = π/4)
(α = 0, β = 0)
(α = −π/4, β = π/4)
0
0.5
1.0
1.5
2.0
2.5
X/δt
β
π/2
π/4
D
A
−π/2
−π/4
α

Figure 4

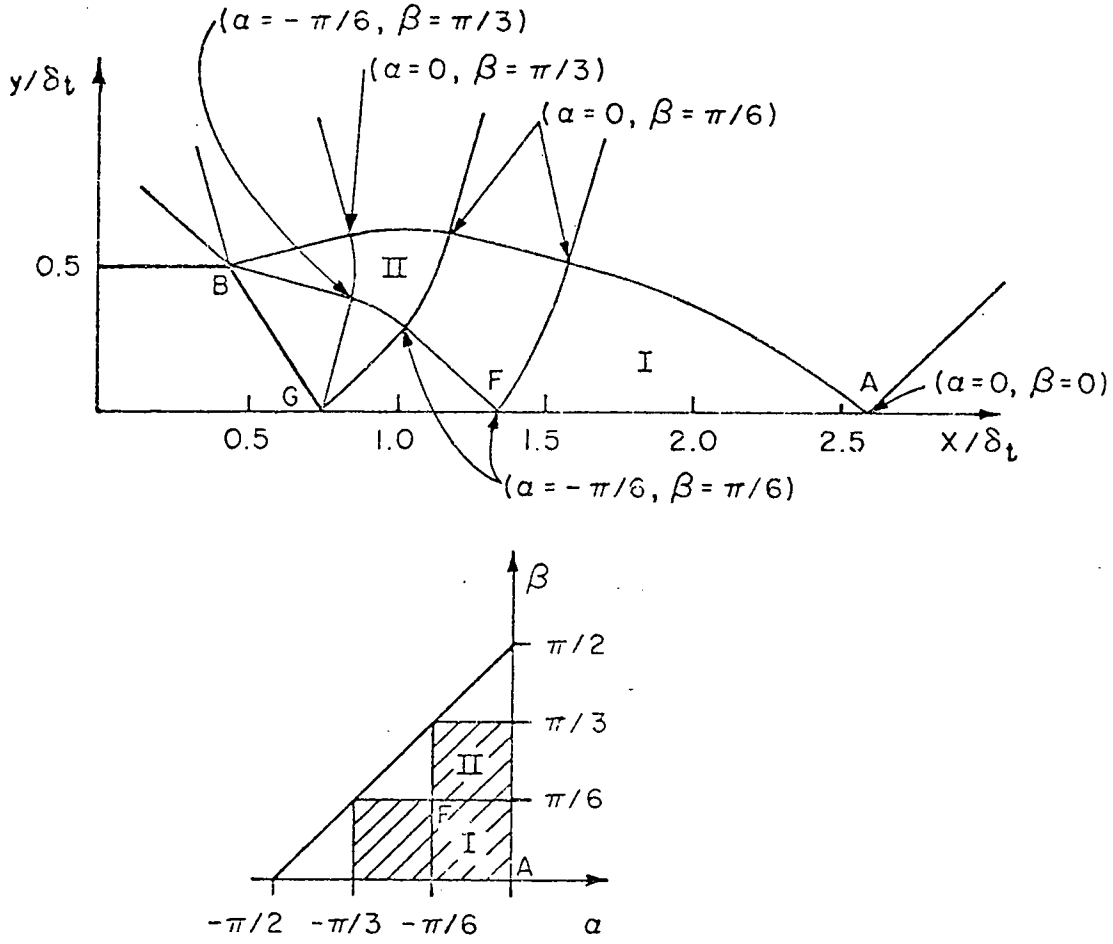
(α = - π/6, β = π/3)
(α = 0, β = π/3)
(α = 0, β = π/6)
y/δt
0.5
B
II
G
F
I
A
(α = 0, β = 0)
0.5
1.0
1.5
2.0
2.5
X/δt
(α = - π/6, β = π/6)
β
π/2
π/3
II
π/6
F
I
A
-π/2
-π/3
-π/6
α

Figure 5

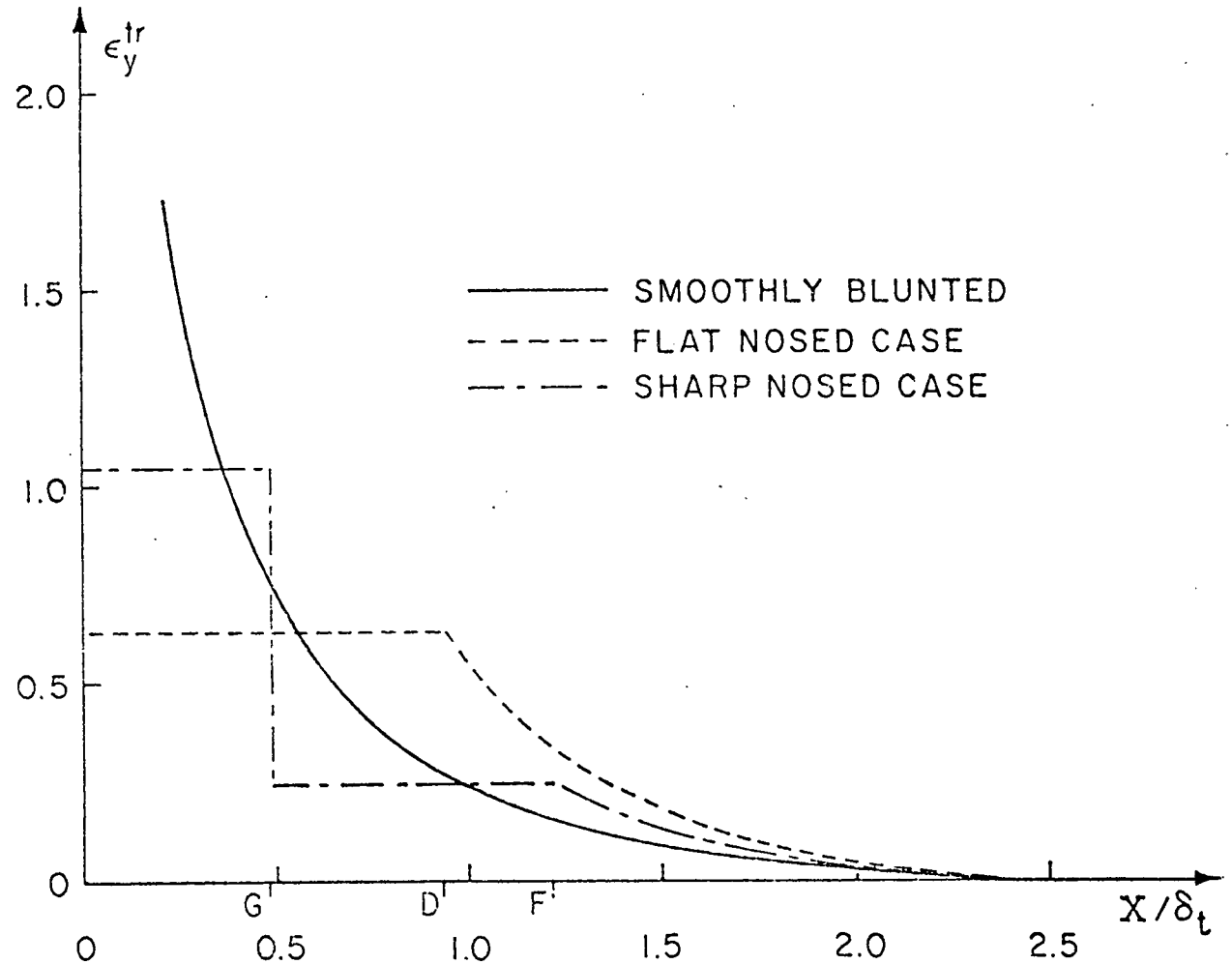
ϵ_y^{tr}
2.0
1.5
1.0
0.5
0
SMOOTHLY BLUNTED
FLAT NOSED CASE
SHARP NOSED CASE
G
D
F
0
0.5
1.0
1.5
2.0
2.5
X/δ_t

Figure 9

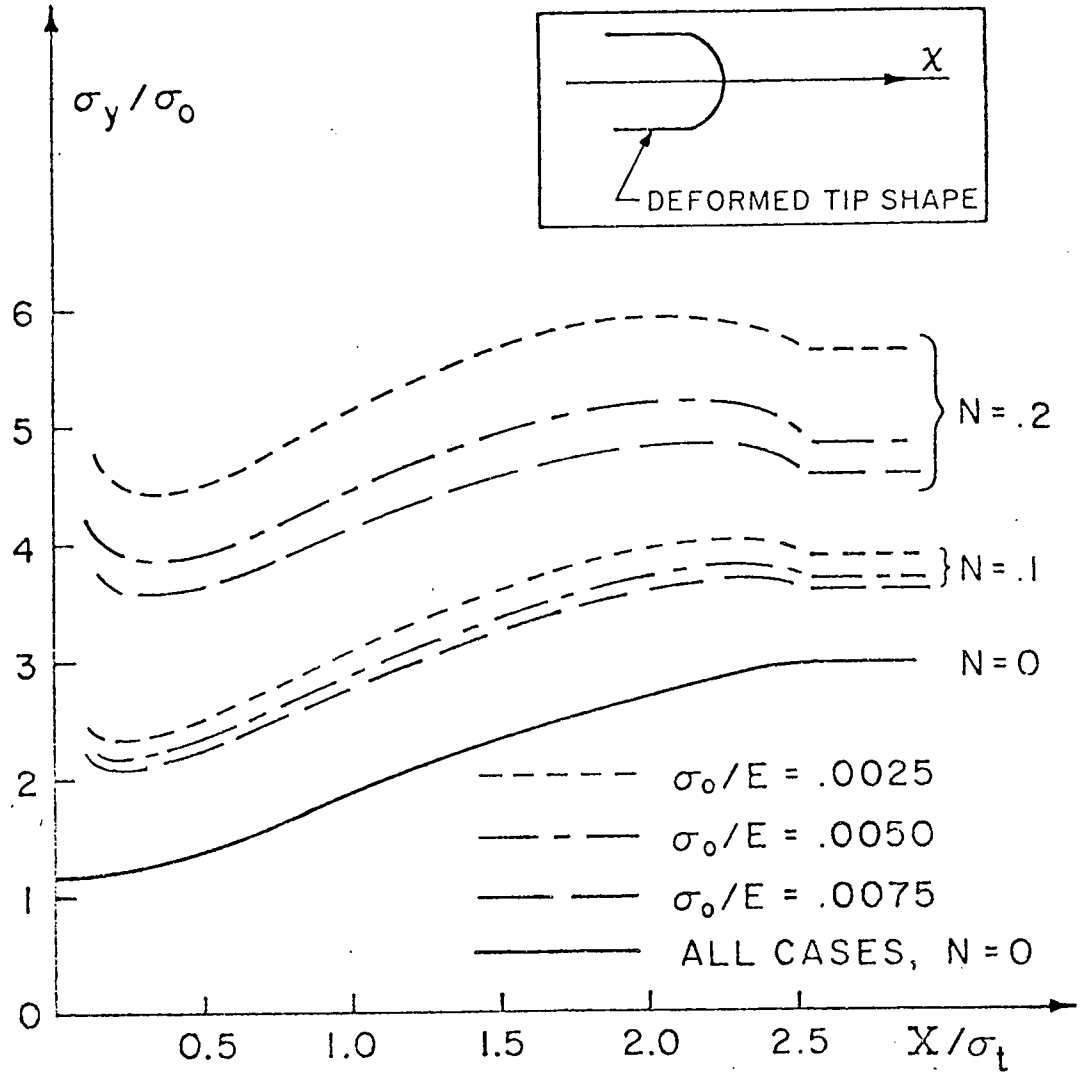
σ_y / σ_0
X
DEFORMED TIP SHAPE
6
5
4
3
2
1
0
N = .2
N = .1
N = 0
σ_0/E = .0025
σ_0/E = .0050
σ_0/E = .0075
ALL CASES, N = 0
0.5
1.0
1.5
2.0
2.5
X/σ_t

Figure 7

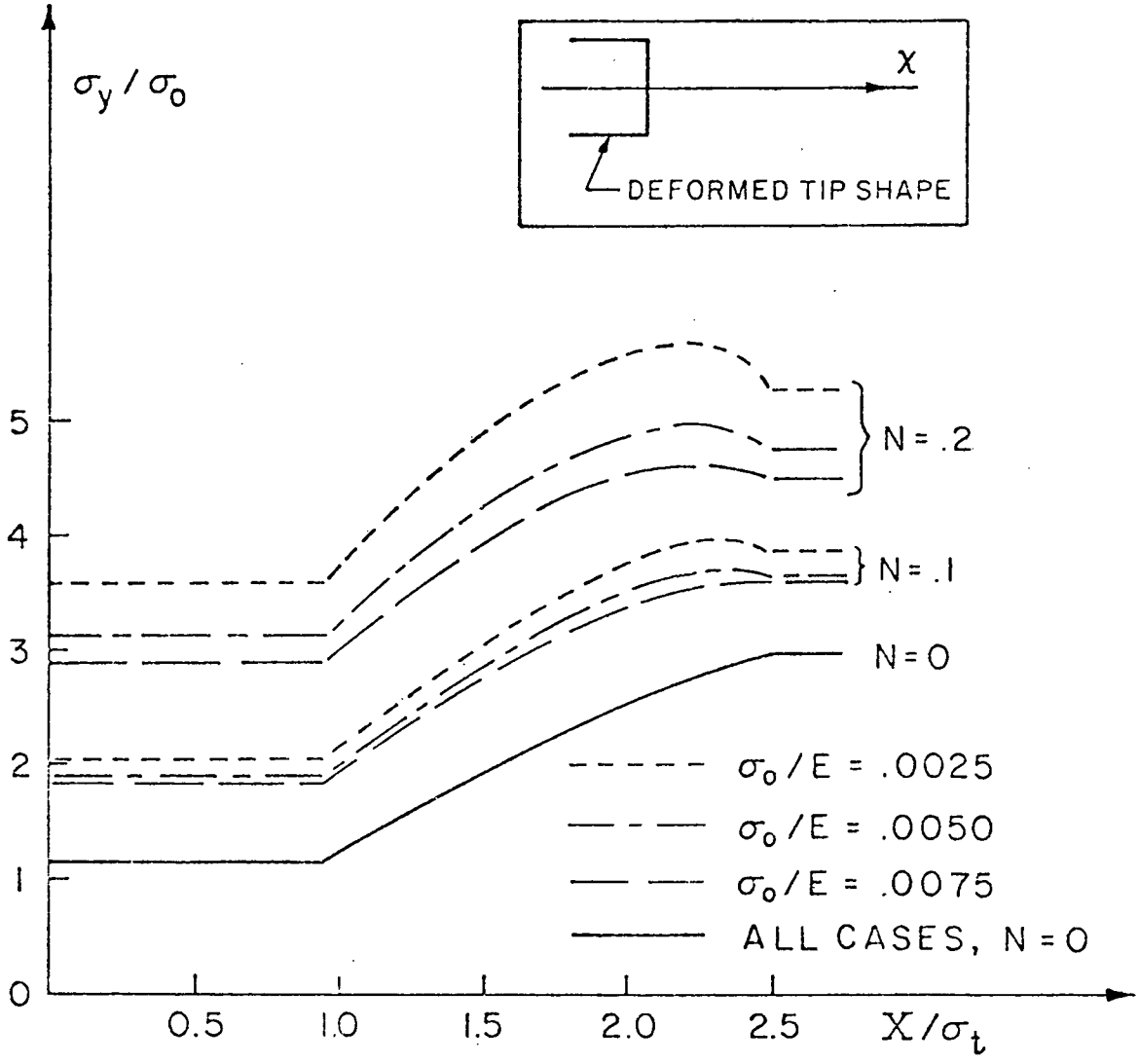
σ_y / σ_0
X
DEFORMED TIP SHAPE
5
4
3
2
1
0
N = .2
N = .1
N = 0
σ_0 / E = .0025
σ_0 / E = .0050
σ_0 / E = .0075
ALL CASES, N = 0
0.5
1.0
1.5
2.0
2.5
X / σ_t

Figure 8

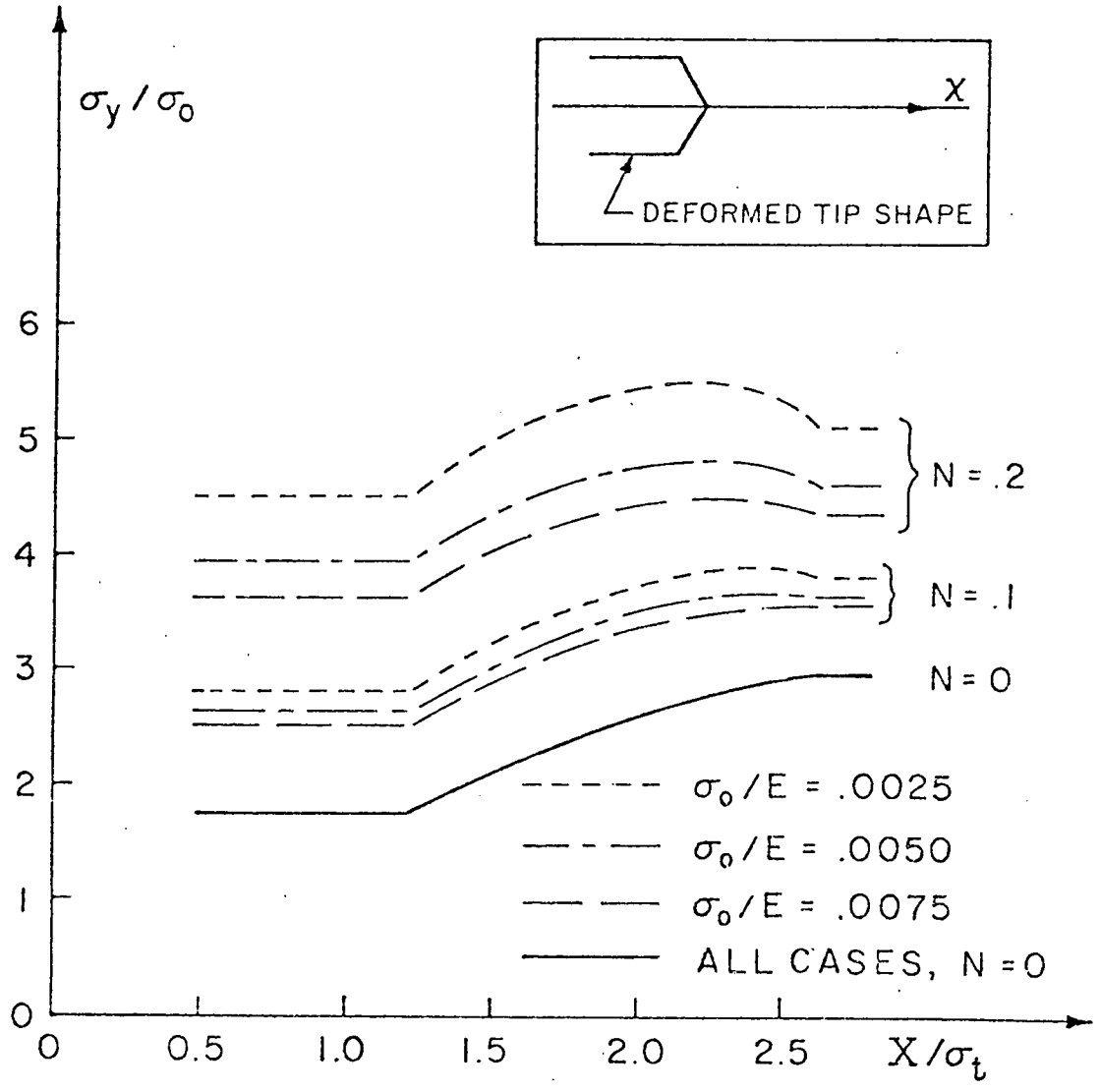
σ_y / σ_0
X
DEFORMED TIP SHAPE
6
5
4
3
2
1
0
N = .2
N = .1
N = 0
σ_0 / E = .0025
σ_0 / E = .0050
σ_0 / E = .0075
ALL CASES, N = 0
0
0.5
1.0
1.5
2.0
2.5
X / σ_t

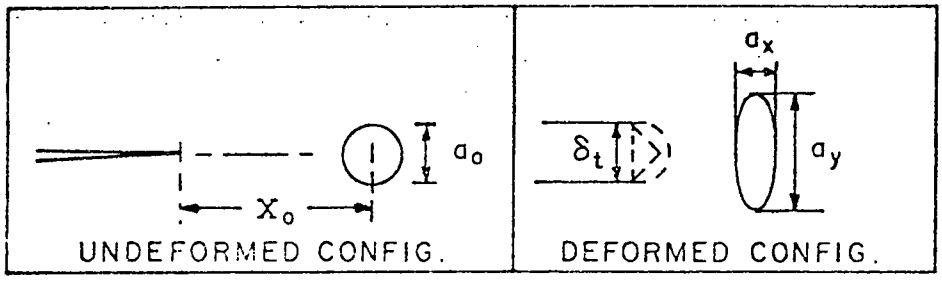
a_o
X_o
UNDEFORMED CONFIG.
a_x
δ_t
a_y
DEFORMED CONFIG.

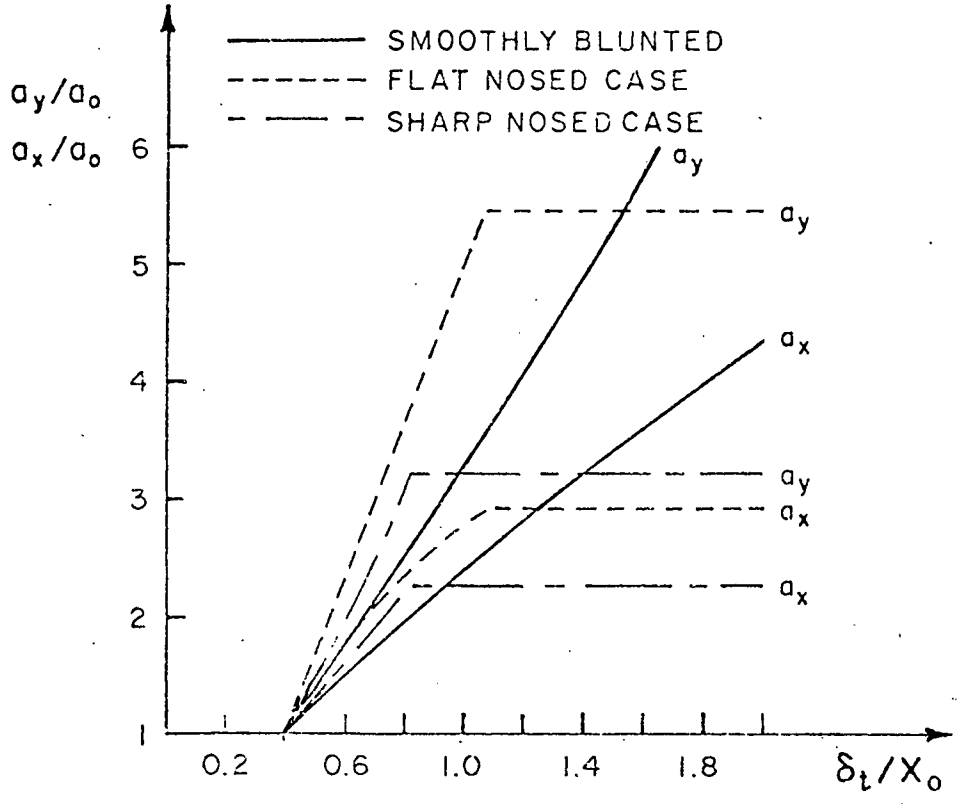
SMOOTHLY BLUNTED
FLAT NOSED CASE
SHARP NOSED CASE
a_y/a_o
a_x/a_o
6
5
4
3
2
1
a_y
a_y
a_x
a_y
a_x
a_x
0.2
0.6
1.0
1.4
1.8
δ_t/X_o

Figure 10

V. LOCALIZATION OF PLASTIC FLOW AT A CRACK TIP AS A MECHANISM FOR THE INITIATION OF PLANE STRAIN DUCTILE FRACTURE *

Summary An unstable localization of plastic flow into a narrow band emenating from a crack tip can arise due to nucleation and the growth of voids. When this occurs, the initiation of fracture follows quite rapidly as the band breaks down. This model for fracture is studied using a macroscopic elastic-plastic constitutive law that accounts for the plastic dilation due to void growth in a hardening material. The localization of plane strain flow occurs when the matrix hardening is no longer sufficient to compensate for the softening due to void growth, and a macroscopic sample of the material reaches a non-hardening state. The hardening rate and mean normal stress of material around a mode I loaded, blunted crack tip in elastic-plastic plane strain may be used to determine the current volume fraction of holes which will allow localization to occur. The current volume fraction of holes may be converted to a volume fraction of void nucleating particles through calculations of the void growth rate near the crack tip. The results indicate that the localization will occur on or near a plane at 45° to the plane of the crack except when the volume fractions of void nucleating particles is small (say, less than 0.01). When the analysis is applied to the fracture behavior of a material, the identification is required of a characteristic distance over which the localization takes place. It would seem to be likely that a lower bound to this distance would be one interparticle spacing of the second phase from which the voids nucleate.

* This is a chapter of the author's Ph.D. thesis, Brown University, June 1977.

INTRODUCTION

It is well established that plastic flow can lozalize into a narrow band of shearing which eventually ruptures. For example, Rogers [1] and Bluhm and Morrisey [2] have observed narrow bands of deformation in the necks of copper tensile specimen just prior to rupture. These bands form in a region that is quite porous. Berg [3] has discussed localization of flow in such porous regions. He suggested that localization would occur when the hardening due to deformation of the matrix is insufficient to overcome the softening due to increasing porosity, and a net macroscopic non-hardening behavior arises. If this mechanism is responsible for the flow localization, it seems likely that the conditions of elevated triaxial stress and substantial plastic strain, that produce localization in necking elastic-plastic tensile specimens, would also cause localization near the tip of a blunted open plane strain crack. Of course, the localization of plastic flow will only occur if no other process of rupture, such as cleavage or gradual coalescence of a neighboring void with the crack, has already taken place. The analysis follows the Berg approach, but is derived from a special case of the work of Rudnicki and Rice [6] on localization of flow in pressure sensitive materials. In this, localization in shear is viewed as a constitutive instability, and the conditions for localization are expressed in terms of the parameters of a constitutive law that can represent plastic dilation. Such a constitutive law has been developed by Gurson [7] for the macroscopic behavior of a material with voids that dilate during plastic flow under the action of a hydrostatic tension. In the absence of the voids, the

constitutive law is the classical Prandtl-Reuss form.

The proper approach to the problem of localization in porous material near a plane strain crack tip would be to formulate the analysis of the near tip deformation with constitutive relations that include the effects of the growing voids. This has not yet been done, even at the approximate level that is represented by Gurson's constitutive law. What is available is McMeeking's [16] analysis of near tip deformation, including the effects of tip blunting, for a plane strain crack tip with contained yielding. The analysis is based on the Prandtl-Reuss constitutive law. If the volume fraction of voids is not too great, McMeeking's results will serve as a reasonable approximation to the state of the matrix of a porous near tip field. Gurson's constitutive law allows one to work out the macroscopic strain hardening rate for a certain volume fraction of holes, when the matrix hardening rate and the hydrostatic stress are known or approximated as just described. By setting the macroscopic hardening rate to zero, which is the appropriate localization condition under the plane strain conditions prevailing near the tip, the current volume fraction of holes necessary to cause localization can be worked out. The void growth rates, as calculated by McMeeking [16] based on the model for void growth of Rice and Tracey [8] and Rice and Johnson [9], can be used to estimate the volume fraction of void nucleating particles (taken identical to the initial volume fraction of holes) that would cause a given current volume fraction of holes. In this way, the model for ductile rupture can be tied to the microscopic features of the material, subject to knowledge of which family of particles provide the voids

involved in the localization process, and over what size scale the localization takes place.

The discussion above, and the development of the model in the next few sections, is based on the idea that a pre-existing porosity leads to a localization of flow when the macroscopic hardening rate of the voided material falls to zero, at least in a state of plane strain. Another, quite separate, point of view may be taken. Rice [4] has suggested that the localization of flow may possibly take place, in the absence of prior hole nucleation and growth, as an inherent instability in the plastic flow process. If the flow localization occurs in the absence of prior hole nucleation and growth, then it is likely that voids will nucleate from particles within the band of intense deformation. These holes would grow and possibly coalesce to cause a rupture in the band. This situation seems to arise in a plastically deformed AISI 4340 steel observed by Cox and Low [5]. A band of intense deformation containing small cavities runs between two larger cavities. There are no signs of porosity on the scale of the smaller cavities on either side of the band of deformation. As shown, for example, in micrographs by Green and Knott [10], localized shearing occurs near crack and notch tips. But, as far as localization of flow of any kind leading to ductile rupture from crack tips is concerned, there is not the same clear direct evidence of it as is available for rupture following localization in tensile specimens as presented by Rogers [1], Bluhm and Morrisey [2] and Cox and Low [5]. However, Rice and Johnson [9] have developed a model for ductile rupture at crack tips due to hole growth which involves the gradual thinning down to zero of the ligament between the crack tip and the void. Fracture data taken from some

materials fits the model quite well, while in other cases the model overpredicts the fracture toughness [9,10,16]. Hahn and Rosenfield [11] and Green and Knott [10] have suggested that in the materials where the fracture toughness is overpredicted, a localization of deformation between the void or an array of voids and the crack tip sets in before the ligament between the void and the crack tip is narrow enough to start thinning down. In addition, Hahn and Rosenfield have noted that in certain aluminum alloys, which have fracture ductilities less than predicted by the model of Rice and Johnson, there is a tendency for plane strain deformation to localize into bands. This localization of flow is present to some extent in all the materials studied by Hahn and Rosenfield.

CONDITION FOR LOCALIZATION OF PLANE STRAIN FLOW IN A PRESSURE SENSITIVE MODEL

The form of constitutive law which can be used to represent pressure sensitivity and plastic dilation is

$$\overset{\nabla}{\sigma}_{ij} = E_{ijk\ell}\left(D_{k\ell} - \frac{1}{h_o} P_{k\ell} Q_{rs} \overset{\nabla}{\sigma}_{rs}\right) , \qquad (1)$$

where $\overset{\nabla}{\underset{\sim}{\sigma}}$ is the Jaumann rate of true stress, $\underset{\sim}{D}$ is the rate of deformation, $\underset{\sim}{E}$ is the tensor of elastic moduli assumed here to correspond to isotropic response with shear modulus G and Poisson ratio ν, h_o is the rate of hardening,

$$P_{ij} = \sqrt{3}\, \sigma'_{ij}/2\bar{\sigma} + (\beta/3)\delta_{ij} ,$$

$$Q_{ij} = \sqrt{3}\, \sigma'_{ij}/2\bar{\sigma} + (\mu/3)\delta_{ij} ,$$

where $\underset{\sim}{\sigma}'$ is the true stress deviator and $\bar{\sigma}^2 = \frac{3}{2}\sigma'_{ij}\sigma'_{ij}$. The term μ is the rate of increase with pressure of the flow stress in shear. Note that if $\mu = \beta = 0$, the constitutive law is the classical Prandtl-Reuss form as discussed by McMeeking and Rice [12].

The approach that Rudnicki and Rice [6] took to the problem of localization was to assume that deformation prior to localization was everywhere homogeneous. The inception of localization was assumed to take place when the strain rate in a narrow planar band could be different from elsewhere. They worked out the kinematic and dynamic conditions for this. This localization can take place even under very constrained boundary conditions [4], so that the bifurcation may be viewed as a constitutive instability rather than a bifurcation of the solution to the governing equations of a finite body deformed by a given set of boundary conditions. But the fact that localization conditions are met does not mean that it will occur. The condition basically allows the growth of a perturbation. The localization condition can be stated as the attainment

of a critical value the hardening modulus, and its value depends on the orientation of the plane of localization relative to the principal stress directions in the homogeneous field. As the material deforms homogeneously prior to localization, the hardening modulus will fall. Thus, the first possible localization is on the plane with the highest associated critical hardening modulus. In plane strain, the value of the hardening modulus that will permit localization of flow is [4]

$$h_o/G = \frac{(1+\nu)^2}{18(1-\nu)} (\mu-\beta)^2 \quad , \qquad (2)$$

where G is the elastic shear modulus and ν is Poisson's ratio for an isotropic material. Note that in deriving this, Rudnicki and Rice neglected rotational effects on the stress rate. This condition, strictly speaking, applies to a plane lying in a homogeneous deformation and stress field. But it seems plausible to apply it to an infinitesimal segment of a curved surface lying in a non-homogeneous field. If the condition for localization is met everywhere on the curved surface, then it would seem possible that localization could arise on the curved surface.

CONSTITUTIVE LAW FOR ELASTIC-PLASTIC MATERIAL WITH VOIDS

The constitutive law developed by Gurson [7] is simply a yield surface and an associated flow rule, but one in which the equivalent yield stress depends on pressure. Gurson utilized a number of approximate flow fields around voids to find approximations to the pressure sensitivity of the yield surface. Gurson's yield surface that will be used here is

$$\phi(\sigma_{ij},\bar{\sigma}_A,f) = \frac{\frac{3}{2}\sigma'_{ij}\sigma'_{ij}}{\bar{\sigma}_A^2} + 2f\cosh\left(\frac{\sigma_{kk}}{2\bar{\sigma}_A}\right) - (1+f^2) = 0 \quad , \qquad (3)$$

where σ_{ij} is the macroscopic state of stress, $\bar{\sigma}_A$ is the volume average tensile flow stress in the matrix material and f is the volume fraction of holes. During a sustained process of plastic flow

$$\frac{\partial\phi}{\partial\sigma_{ij}}\overset{\nabla}{\sigma}_{ij} + \frac{\partial\phi}{\partial\bar{\sigma}_A}\dot{\bar{\sigma}}_A + \frac{\partial\phi}{\partial f}\dot{f} = 0 \quad , \qquad (4)$$

which follows from the consistency condition ($\dot{\phi} = 0$). The macroscopic rate of stress working per unit volume, $\sigma_{ij}D_{ij}$, where $\underset{\sim}{D}$ is the macroscopic rate of deformation, is equal to the rate of stress working in the matrix material. The average equivalent strain rate in the matrix material may be approximated by $\dot{\bar{\sigma}}_A/h$, where h is the volume average hardening rate of the matrix material. Then the rate of stress working per unit macroscopic volume is $\dot{\bar{\sigma}}_A\bar{\sigma}_A(1-f)/h$ and so [7]

$$\dot{\bar{\sigma}}_A = \frac{h\sigma_{ij}D_{ij}}{\bar{\sigma}_A(1-f)} \quad .$$

When one takes note of the kinematic relation

$$\dot{f} = (1-f)D_{kk} \quad ,$$

and that Berg [3] and Gurson [7] following Bishop and Hill [17], have argued that a flow rule of the form

$$D^p_{ij} = \Lambda \frac{\partial \phi}{\partial \sigma_{ij}} \quad ,$$

where $\underset{\sim}{D}^p$ is the plastic part of $\underset{\sim}{D}$, may be applied to a macroscopic element of porous material, it follows that

$$D^p_{ij} = \frac{1}{H} \frac{\partial \phi}{\partial \sigma_{ij}} \frac{\partial \phi}{\partial \sigma_{k\ell}} \overset{\nabla}{\sigma}_{k\ell} \quad , \qquad (6)$$

where

$$H = \left\{ \left[f \sinh\left(\frac{\sigma_{kk}}{2\bar{\sigma}_A}\right)\left(\frac{\sigma_{kk}}{2\bar{\sigma}_A}\right) + (1+f^2) - 2f \cosh\left(\frac{\sigma_{kk}}{2\bar{\sigma}_A}\right) \right]^2 \left(\frac{4h}{\bar{\sigma}_A^2(1-f)}\right) \right.$$

$$\left. + \frac{6(1-f)f}{\bar{\sigma}_A} \left[\cosh\left(\frac{\sigma_{kk}}{2\bar{\sigma}_A}\right) - f \right] \sinh\left(\frac{\sigma_{kk}}{2\bar{\sigma}_A}\right) \right\} .$$

Note that $\partial\phi/\partial\sigma_{ij}$ has exactly the form of P_{ij} and Q_{ij} to within scalar multiplying factors. All that is required to get (6) into the form of (1) is to add an elastic reponse to (6) and rearrange terms. It is then obvious that in this constitutive law $P_{ij} = Q_{ij}$. As a consequence $\mu = \beta$, and $h_o = 0$ in (2) will permit localization of flow to take place. This means that $H = 0$ is a condition that permits the localization of flow in plane strain for the materials with yield given by (3). In terms of the matrix hardening rate, the localization condition is

$$\frac{h_{crit}}{\bar{\sigma}_A} = \frac{6(1-f)^2 f \left[\cosh\left(\frac{\sigma_{kk}}{2\bar{\sigma}_A}\right) - f \right] \sinh\left(\frac{\sigma_{kk}}{2\bar{\sigma}_A}\right)}{\left[2(1+f^2) - 4f \cosh\left(\frac{\sigma_{kk}}{2\bar{\sigma}_A}\right) + \frac{\sigma_{kk}}{\bar{\sigma}_A} f \sinh\left(\frac{\sigma_{kk}}{2\bar{\sigma}_A}\right) \right]^2} \cdot \qquad (7)$$

This relationship has been plotted in fig. 1 as $h_{crit}/\bar{\sigma}_A$ versus $\sigma_{kk}/\bar{\sigma}_A$ for various volume fractions of holes, f . The larger the value of h_{crit} is, the earlier, in terms of strain, the localization will take place. The material with a larger volume fraction of holes is less stable, and the more hydrostatic tension that is applied, the sooner localization will take place.

The development in this section is taken from an earlier discussion by Rice [18].

LOCALIZATION AT A CRACK TIP

The result (7) may be used to calculate the volume fraction of holes required to allow localization to take place near a loaded crack tip in contained plane strain yielding. The results of the finite element solution of McMeeking [16] are suitable for providing the near tip stress and deformation field around a blunted crack tip. This analysis was carried out using the Prandtl-Reuss equations, and a hardening law of the form

$$(\bar{\tau}/\sigma_o)^{1/N} = (\bar{\tau}/\sigma_o) + 3G\bar{\varepsilon}^p/\sigma_o \quad ,$$

where $\bar{\tau}^2 = \frac{3}{2}\tau'_{ij}\tau'_{ij}$, $\underset{\sim}{\tau}'$ is the Kirchhoff stress deviator, $\underset{\sim}{\tau} = |F|\underset{\sim}{\sigma}$ where $|F|$ is the ratio of volume of a material element in the current state to its volume in the undeformed state, $\underset{\sim}{\sigma}$ is the true stress tensor, σ_o is the tensile yield stress in terms of Kirchhoff stress and G is the elastic shear modulus. Note that $\bar{\varepsilon}^p = \int\left(\frac{2}{3}D^p_{ij}D^p_{ij}\right)^{1/2}dt$, where $\underset{\sim}{D}^p$ is the plastic part of the rate of deformation tensor $D_{ij} = \left(\partial v_i/\partial x_j + \partial v_j/\partial x_i\right)/2$, where $\underset{\sim}{v}$ is velocity, $\underset{\sim}{x}$ is the current material position and t is time. The results for the material with $N = 0.1$ and $\sigma_o/E = 1/300$, where E is Young's modulus, was chosen for the localization analysis. The near tip stress and plastic strain for this case is shown in fig. 2, which is taken from [16].

The terms σ_{kk} , $\bar{\sigma}_A$ and h_{crit} in (7) will be simply equated to the sum of the normal stresses, the flow stress and the hardening rate (known as a function of local equivalent plastic strain or stress $\bar{\sigma}_A$) in the finite element solution. This is somewhat approximate, but in the absence of the solution that takes into account the presence of the holes, it will suffice. With all other terms known, f may be

evaluated in (7) by a trial and error approach. The values of f that will allow localization to occur around the crack tip are shown in fig. 3 where the loci are drawn in the undeformed configuration. As can be seen, the closer a point is to the crack tip, with distance phrased as multiples of the current crack tip opening displacement, b, the smaller the volume fraction of holes that is required to allow localization to take place. This reflects the fact that there is an area of high triaxial stress and large plastic strain near the crack tip, as discussed by Rice and Johnson [9] and McMeeking [16].

Since the near tip stress and deformation field does not change in magnitude, after sufficient opening, but spreads out as the crack tip opening displacement is increased, localization can occur for very small crack tip opening displacements, unless the conditions for localization are required to prevail over a characteristic finite distance before the failure takes place. That means that localization would occur at an angle of about 45° to the X-axis if the current (versus initial) volume fraction of voids were fairly evenly spread over the crack tip region. For localization to occur on the plane of symmetry, there would have to be a much greater concentration of voids there than elsewhere.

An approximate calculation of the volume fraction of voids in the undeformed configuration, before load is applied to the cracked body, may be made using fig. 4, which is taken from [16]. This figure is the result of using the void growth model of Rice et al. [8,9] to calculate the ratio of deformed to undeformed size of an originally spherical void growing in the near tip region. Only information for the X-axis

and the line at 45° to the X-axis is available from fig. 4. The horizontal scale in fig. 4 is the inverse of the distance of the position of the void in the undeformed configuration from the crack tip, measured in units of current crack tip opening displacements. In addition, the ratio of current void volume fraction to undeformed volume fraction

$$f/f_o = (a_1 a_2/a_o^2)^{3/2} \quad ,$$

since the void is deformed into an ellipsoid with dimensions a_1, a_2 and $\sqrt{a_1 a_2}$. Using this, fig. 3 may be converted into another diagram of the same type, but concerned with f_o, rather than f, if fuller information on void growth rates was available. Instead, fig. 5 has been drawn, which is a plot of the crack opening displacement at the time localization can first occur, measured in units of the characteristic distance over which localization takes place, as a function of the volume fraction of holes in the undeformed configuration for the two void positions for which results are available. The void growth calculations in [16] are for a void which starts growing as soon as it enters the plastic zone. That means that f_o in fig. 5 can be interpreted as the critical volume fraction of particles which nucleate cavities around themselves after negligible amounts of plastic deformation. As such, the usefulness of fig. 5 is somewhat restricted, and an improvement would come from incorporating a nucleation criterion in the calculations.

It is of interest that over most of the range of f_o plotted in fig. 5, the localization is predicted to occur at or near 45° to the axis of symmetry. This means that the first amount of crack growth due to this type of ductile rupture in materials with a volume fraction of void

nucleating particles larger than about .01 is predicted to be angled crack growth. It is only at the lower volume fractions of void nucleating particles that a changeover to straight ahead growth occurs. It is difficult to estimate where the changeover takes place in terms of f_o and it will, of course, be spread over some range of f_o as the crack growth direction gradually approaches the axis of symmetry. Berg [3] has indicated that localization of flow in a porous material is a mechanism by which an advancing crack can zig-zag. Van den Avyle [13] has observed zig-zag crack growth in fracture toughness specimens of 4340 and maraging 300 steel. He noted that the wavelength of the zig-zag growth could be correlated with K_{Ic} . This would seem to fit in with the concept of ductile rupture due to lo-localization of flow initiating over a characteristic distance once the crack tip opening displacement is large enough. Of course, once the crack has grown out of the region near the blunted open crack tip, the analysis just described is not relevant. Another point is that Van den Avyle observed no general porosity, so it is not clear what role porosity plays in the fracture process in these steels. However, Cox and Low [5] have observed the nucleation of holes, their growth and coalescence in the same alloys. But the observations are not conclusive as to what mechanism causes the localization of flow in such materials (that is, it is not clear whether porosity or some instability of the plastic flow within the unvoided matrix causes the localization).

The development so far has concerned only one value of the hardening exponent, N . To properly compare the behavior of different materials, the dependence of the behavior on the hardening exponent should, of course, be taken into account. That the localization of flow

due to pre-existing porosity depends on the hardening rate is obvious by considering a matrix material that does not harden. In that case, a macroscopic element containing growing voids will experience strain softening. It follows that the condition for localization of flow in plane strain, namely, that the macroscopic hardening rate be zero or less, will be met as soon as voids start to grow. Thus, a non-hardening matrix material would allow rupture from a crack tip due to localized flow as soon as enough voids were nucleated around the crack tip to give rise to a macroscopic porosity. The critical crack tip opening displacement at the onset of fracture would probably be much smaller in a specimen in which the matrix material is non-hardening compared to the critical COD in a specimen made from a matrix material that hardens. To fully establish the dependence of fracture toughness on the strain hardening exponent in this model would require results intermediate to $N = 0$ and $N = 0.1$. The deduction from the results for $N = 0$ and $N = 0.1$ fits in with the suggestion by Krafft [19] that the plane strain fracture toughness correlates directly with N in a number of materials that fail by ductile rupture. His correlation involves a zero toughness when $N = 0$, a somewhat unreasonable result, but it presumably really indicates a dramatic reduction of the toughness in the non-hardening materials.

COMPARISON OF LOCALIZATION MODEL RESULTS WITH SOME DATA FOR ALUMINUM ALLOYS

Van Stone, Merchant and Low [14] have carried out an extensive metallographic analysis of some 2000 and 7000 series high strength aluminum alloys. They also provided some mechanical properties of the alloys, such as plane strain fracture toughness, yield strength and hardening exponent. Van Stone et al. observed that rupture in these alloys commenced with voids nucleating from a family of large particles. These voids grew and eventually coalesced, and they would presumably coalesce with the crack tip if they were sufficiently near, constituting the ductile rupture that is suggested by the fracture surface appearance. Rice [20] has calculated the critical crack tip opening displacement at fracture from the data of Van Stone et al., and concluded that it is approximately equal to the average nearest neighbor spacing of the particles which first nucleate voids. McMeeking [16] has used the data in [14,20] to plot the critical crack tip opening displacement at fracture versus the spacing of the void nucleating particles. The critical COD is normalized by the spacing of the void nucleating particles, and on the other scale the spacing of the void nucleating particles is normalized by their diameter. According to a model due to Rice and Johnson [9] involving the growth of voids and their gradual coalescence with the crack tip, the COD to particle spacing ratio can be related to the spacing to diameter ratio. But the model overestimates the critical COD by a factor of about 2 in the 7000 series aluminums while it predicts the critical COD for the 2000 series quite well. Hahn and Rosenfield [11] have suggested that a localization of flow in the near tip region, leading

to rupture, intervenes in the 7000 series alloys before the void starts to gradually coalesce with the crack tip. As a result, the critical COD at the onset of fracture is less than that predicted by the model of Rice and Johnson.

It is possible that the localization of flow is porosity induced. To aid an investigation of this, some data for the alloys have been tabulated. Some of the data is based on the model for ductile rupture due to porosity induced flow localization, as represented by fig. 5. This model is based on results for a material with power law hardening exponent N, of 0.1 and a uniaxial tensile yield strain of 1/300. As such, the development below takes no account of the influence of the different hardening properties of each alloy, although hardening properties would seem to play an important, if not dominant role in the rupture caused by porosity induced flow localization.

In the Table, the alloys are listed along with f_o, the volume fraction of particles that Van Stone et al. observed to nucleate voids. From f_o, the ratio of crack tip opening displacement to characteristic distance, b/X_o, at the first possibility of localization of flow due to porosity can be inferred from fig. 5 and the results are entered in the Table. Finally, the ratio of crack tip opening displacement at fracture, b, to the planar nearest neighbor spacing of the particles from which the holes nucleate, D, can be calculated from the data in [14]. This allows calculation of X_o/D, the ratio of the inferred characteristic distance for localization to occur to the planar nearest neighbor spacing of the particles. As can be seen from the Table, the inferred characteristic distance in the 2000 series alloys is 2 to 3 times the planar nearest neighbor spacing of the particles from which voids nucleate. However, the

7000 series alloys suggest a smaller number, of the order of the planar nearest neighbor spacing. Additionally, since Rice [20] deduced the three dimensional nearest neighbor spacing of the void nucleating particles to be approximately equal to the critical crack tip opening displacement, the inverse of the predicted b/X_o values in the Table gives the ratio of X_o to the three dimensional nearest spacing of the particles. This means that the inferred characteristic distance is approximately 2 to 3 times the three dimensional nearest neighbor spacing of the void nucleating particles. It is not clear which spacing of the particles, planar or three dimensional, would be significant to the localization process. However, if it is assumed that a localization of flow can take place if the conditions for localization are met over an area including, very roughly, 2 to 3 three dimensional interparticle spacings, then localization of flow due to pre-existing porosity could have caused the rupture in both the 2000 and 7000 series alloys. Similarly, the behavior of the 2000 series alloy could be predicted if localization conditions had to be met over two planar interparticle spacings before rupture takes place. But this would overestimate the toughness of the 7000 series alloys. The conclusion would seem to be that localization of flow of the Berg type is unlikely to be causing the rupture in both 2000 series and 7000 seris alloys, if indeed it causes the rupture in either one or the other series of alloys. Of course, these comments are based on a model which, as yet, takes no account of the differences in yield strength and hardening behavior of the different alloys. As discussed already, the hardening properties of the alloy would influence the localization behavior quite

significantly. The 2000 series alloys that Van Stone et al. used in their study all have hardening exponents that are smaller than the hardening exponents of the 7000 seris alloys, which were closer to 0.1. Since smaller hardening exponents would probably lead to earlier localization, the fracture behavior of the alloys is more difficult to resolve with a porosity-localization model than the tablulated data suggest. As a result, it seems fair to conclude that if localization of flow does explain the fracture behavior of the aluminum alloys discussed, the localization does not arise due to porosity in both series of alloys. If localization of flow due to the porosity mechanism occurs in either type of alloy, it would seem only possible that it occurs in the 2000 series alloys. If localization of flow occurs in the 7000 series alloys, it would appear that it arises from some instability of the plastic flow not due to "porosity softening."

CONCLUSIONS

An approximate approach to incorporating the effect of porosity on the macroscopic hardening rate of material near a blunted crack tip, loaded by mode I type loads, indicates that localization of flow can occur near the crack tip. The localization of flow will cause some crack growth at an angle to the plane of the crack by preference to straight-ahead growth, at least for a certain range of volume fractions of void nucleating particles. The hardening properties of the material will greatly influence the tendency for localization of flow due to porosity to occur. If the matrix material is non-hardening, the localization could occur as soon as plastic straining occurs if voids are already present. This would seem to be in agreement with an observed correlation of increasing toughness with increasing hardening exponent.

ACKNOWLEDGEMENT

The author is indebted to Professor J. R. Rice for helpful discussions of this topic. The author received support from the U. S. Energy Research and Development Administration under contract E(11-1)3084 to carry out this work.

REFERENCES

[1] Rogers, H. C., Transactions of the Metallurgical Society of the AIME, 218, 1960, p. 498.

[2] Bluhm, J. I., and Morrisey, R. J., in Proceedings of the 1st International Conference on Fracture, T. Yokobori et al. Eds., Japanese Society for Strength and Fracture of Materials, Vol. 3, 1966, pp. 1739-1780.

[3] Berg, C. A., in Inelastic Behavior of Solids, M. F. Kanninen et al. Eds., Mc-Graw Hill, New York, 1970, pp. 171-209.

[4] Rice, J. R., "The Localization of Plastic Deformation," in Theoretical and Applied Mechanics (Proceedings of the 14th International Congress on Theoretical and Applied Mechanics, Delft, 1976, Edited by W. T. Koiter), North-Holland, Vol, 1, 1976, pp. 207-220.

[5] Cox, T. B., and Low, J. R., Metallurgical Transactions, 5, 1974, pp. 1457-1470.

[6] Rudnicki, J. W., and Rice, J. R., Journal of the Mechanics and Physics of Solids, 23, 1975, pp. 371-394.

[7] Gurson, A. L., "Continuum Theory of Ductile Rupture by Void Nucleation and Growth; Part I - Yield Criteria and Flow Rules for Porous Ductile Media." To appear in Transactions of the A.S.M.E. (Series H, Journal of Engineering Materials and Technology).

[8] Rice, J. R., and Tracey, D. M., Journal of the Mechanics and Physics of Solids, 17, 1969, p. 201.

[9] Rice, J. R., and Johnson, M. A., in Inelastic Behavior of Solids, M. F. Kanninen et al. Eds., McGraw-Hill, New York, 1970, p. 641.

[10] Green, G., and Knott, J. F., Transaction of the ASME (Series H, Journal of Engineering Materials and Technology) 98, 1976, p. 37.

[11] Hahn, G. T., and Rosenfield, A. R., Metallurgical Transactions, 6A, 1975, p. 653.

[12] McMeeking, R. M., and Rice, J. R., International Journal of Solids and Structures, 11, 1975, p. 601.

[13] Van den Avyle, J. A., Ph.D. Dissertation, Massachusetts Institute of Technology, 1975.

[14] Van Stone, R. H., Merchant, R. M., and Low, J. R., in A.S.T.M., S.T.P. 556, p. 93.

[15] Gurson, A. L., Ph.D. Dissertation, Brown University, 1975.

[16] McMeeking, R. M., "Finite deformation analysis of crack tip opening and implications for fracture initiation," Technical Report E(11-1)3084/44, Division of Engineering, Brown University, Providence, R. I., May 1976, also Ph.D. Dissertation, Brown University, 1976.

[17] Bishop, J. F. W., and Hill, R., Philosophical Magazine, 42, 1951, p. 414.

[18] Rice, J. R., private communication with A. L. Gurson, 1972.

[19] Krafft, J. M., Applied Materials Research, 3, 1964, p. 88.

[20] Rice, J. R., "Elastic-Plastic Fracture Mechanics," in The Mechanics of Fracture, Ed. F. Erdogan, American Society of Mechanical Engineers, New York, 1976, in press.

TABLE

Alloy	f_o	b/X_o	b/D	X_o/D
2014-T6	.029	.28	.62	2.2
2024-T851	.027	.29	.77	2.7
2124-T851	.010	.42	.87	2.1
7075-T7351	.004	.61	.85	1.4
7079-T651	.004	.61	.62	1.0

LIST OF FIGURE CAPTIONS

Fig. 1 The volume average rate of hardening of the matrix in a material with voids that allow localization of flow into a narrow band as a function of the sum of the normal stresses, σ_{kk}, and of the volume fraction of holes, based on Gurson's [7] constitutive law.

Fig. 2 Plot of stress $\sigma_{\theta\theta}/\sigma_o$ and plastic strain around the loaded blunted crack tip for $\sigma_o/E = 1/300$ and $N = 0.1$. Note σ_o is the yield stress in tension and R and θ are defined for the position of the material in the undeformed configuration.

Fig. 3 Current volume fraction of voids, f, that is sufficiently large to allow the localization of flow in the stress and deformation field around a blunted notch tip of width b. The material has a tensile yield strain of 1/300 and a hardening exponent of 0.1. The loci are drawn in the undeformed configuration.

Fig. 4 Plot of dimensions of a void, growing in the near tip field in the material with $\sigma_o/E = 1/300$ and $N = 0.1$, versus the crack tip opening displacement. The void starts growing as soon as it enters the plastic zone.

Fig. 5 Ratio of crack tip opening displacement b to characteristic distance X_o over which localization occurs as a function of the volume fraction of particles f_o, which nucleate the holes that induce localization of flow near the crack tip.

sm

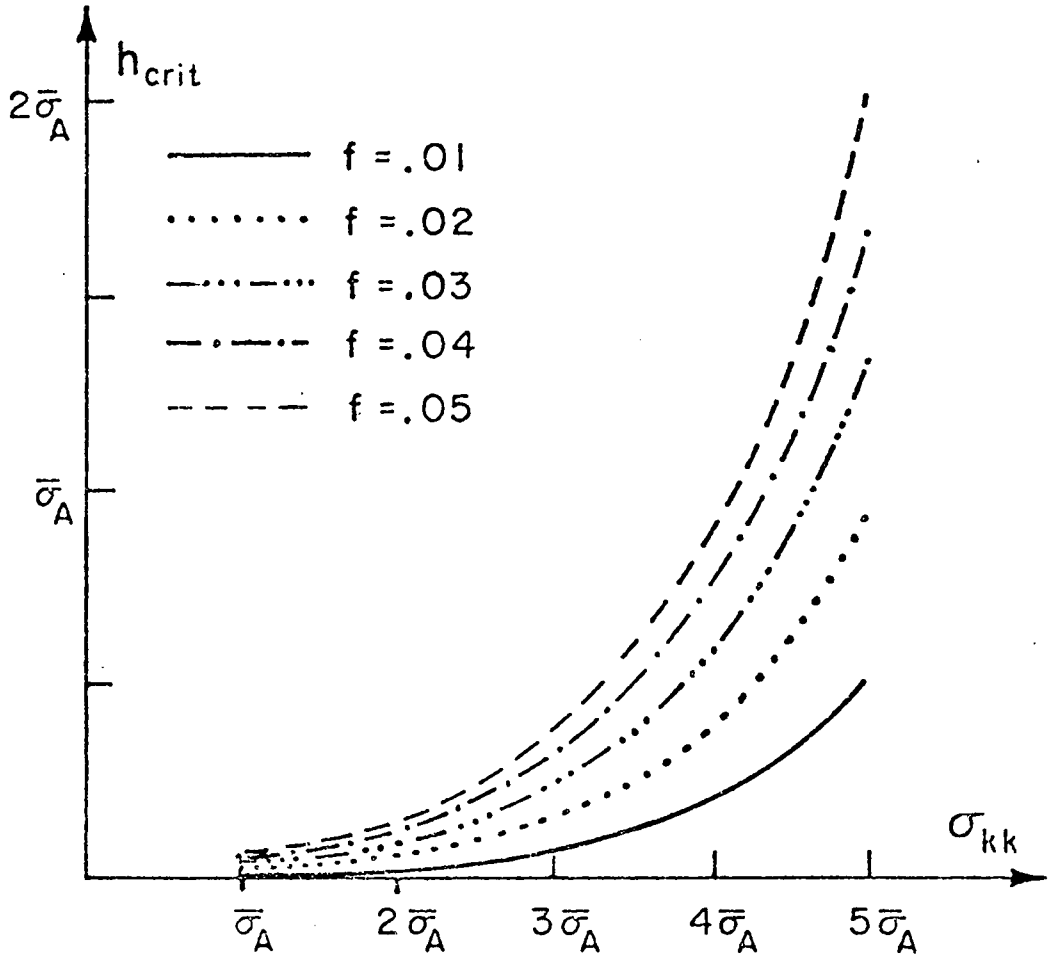
h_{crit}
$2\bar{\sigma}_A$
$\bar{\sigma}_A$
f = .01
f = .02
f = .03
f = .04
f = .05
σ_{kk}
$\bar{\sigma}_A$
$2\bar{\sigma}_A$
$3\bar{\sigma}_A$
$4\bar{\sigma}_A$
$5\bar{\sigma}_A$

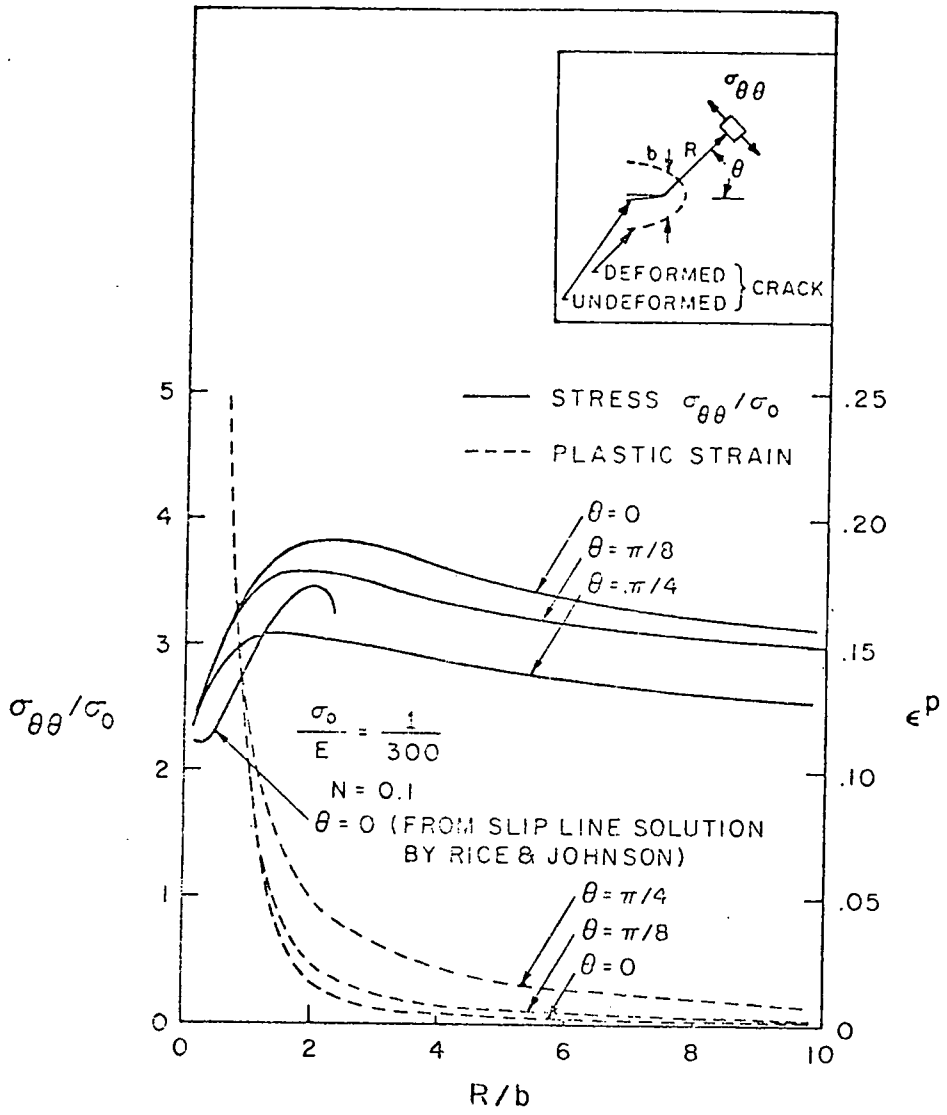
$\sigma_{\theta\theta}$
b
R
θ
DEFORMED
UNDEFORMED
CRACK
STRESS $\sigma_{\theta\theta}/\sigma_0$
PLASTIC STRAIN
θ = 0
θ = π/8
θ = π/4
$\frac{\sigma_0}{E} = \frac{1}{300}$
N = 0.1
θ = 0 (FROM SLIP LINE SOLUTION BY RICE & JOHNSON)
θ = π/4
θ = π/8
θ = 0
$\sigma_{\theta\theta}/\sigma_0$
ϵ^p
R/b
0
1
2
3
4
5
0
2
4
6
8
10
.05
.10
.15
.20
.25

Figure 2

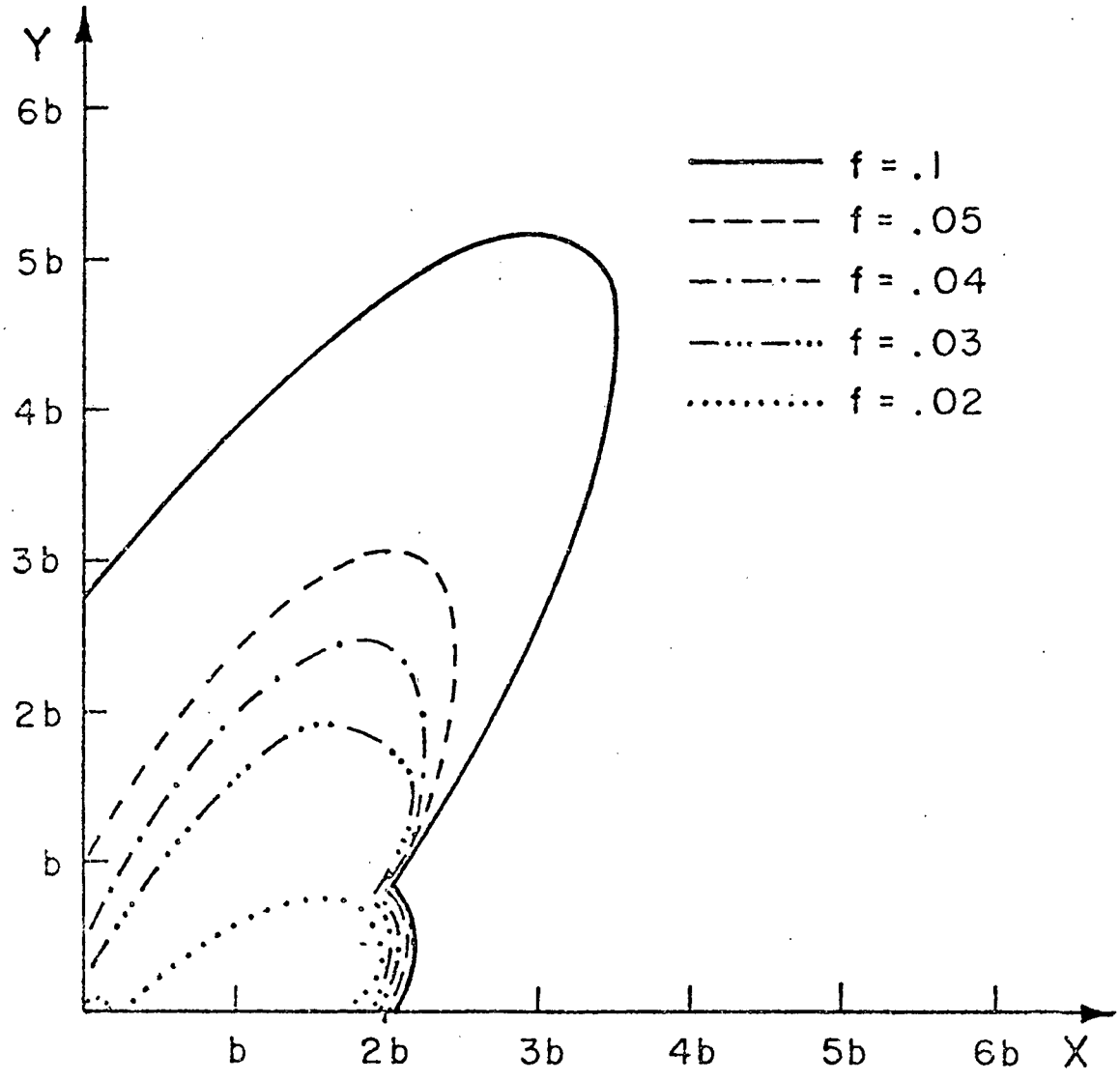

Figure 3

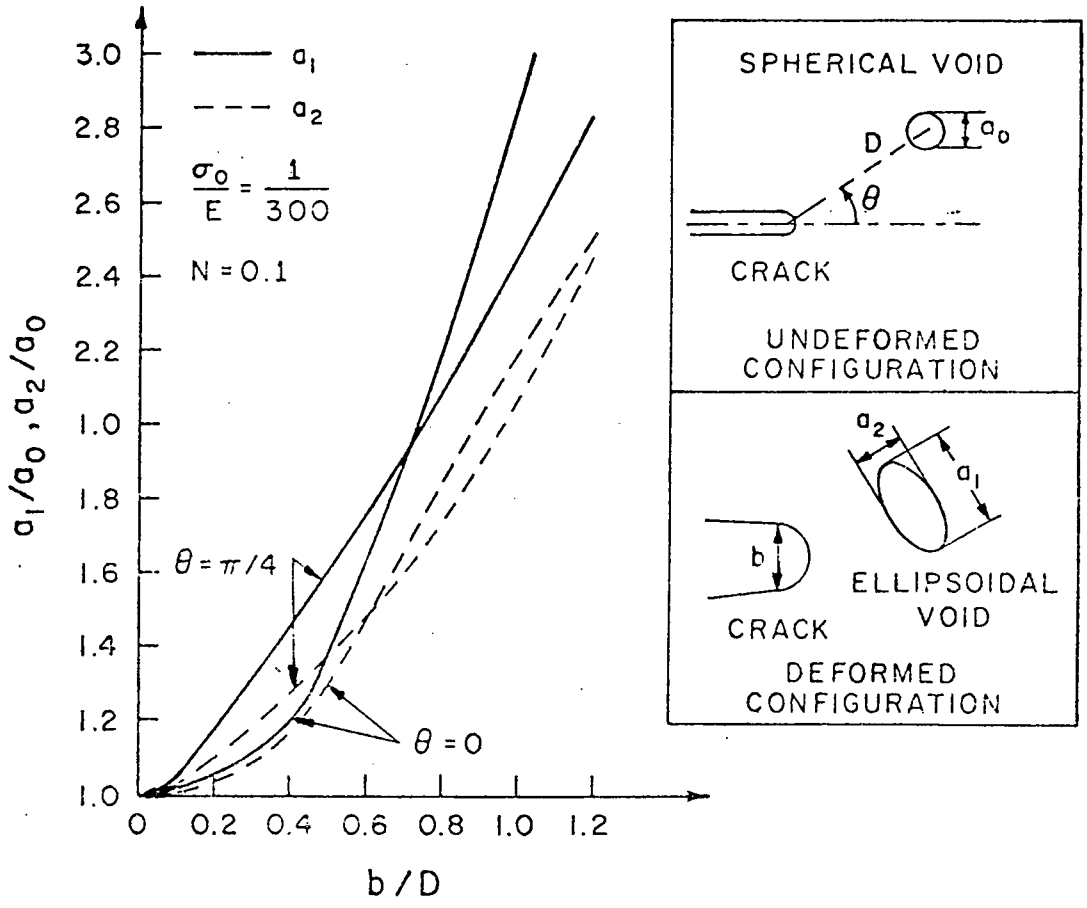
3.0
2.8
2.6
2.4
2.2
1.0
1.8
1.6
1.4
1.2
1.0
a_1
a_2
$\frac{\sigma_0}{E} = \frac{1}{300}$
N = 0.1
$\theta = \pi/4$
$\theta = 0$
0
0.2
0.4
0.6
0.8
1.0
1.2
b/D
a_1/a_0 , a_2/a_0
SPHERICAL VOID
D
a_0
θ
CRACK
UNDEFORMED CONFIGURATION
a_2
a_1
b
CRACK
ELLIPSOIDAL VOID
DEFORMED CONFIGURATION

Figure 4

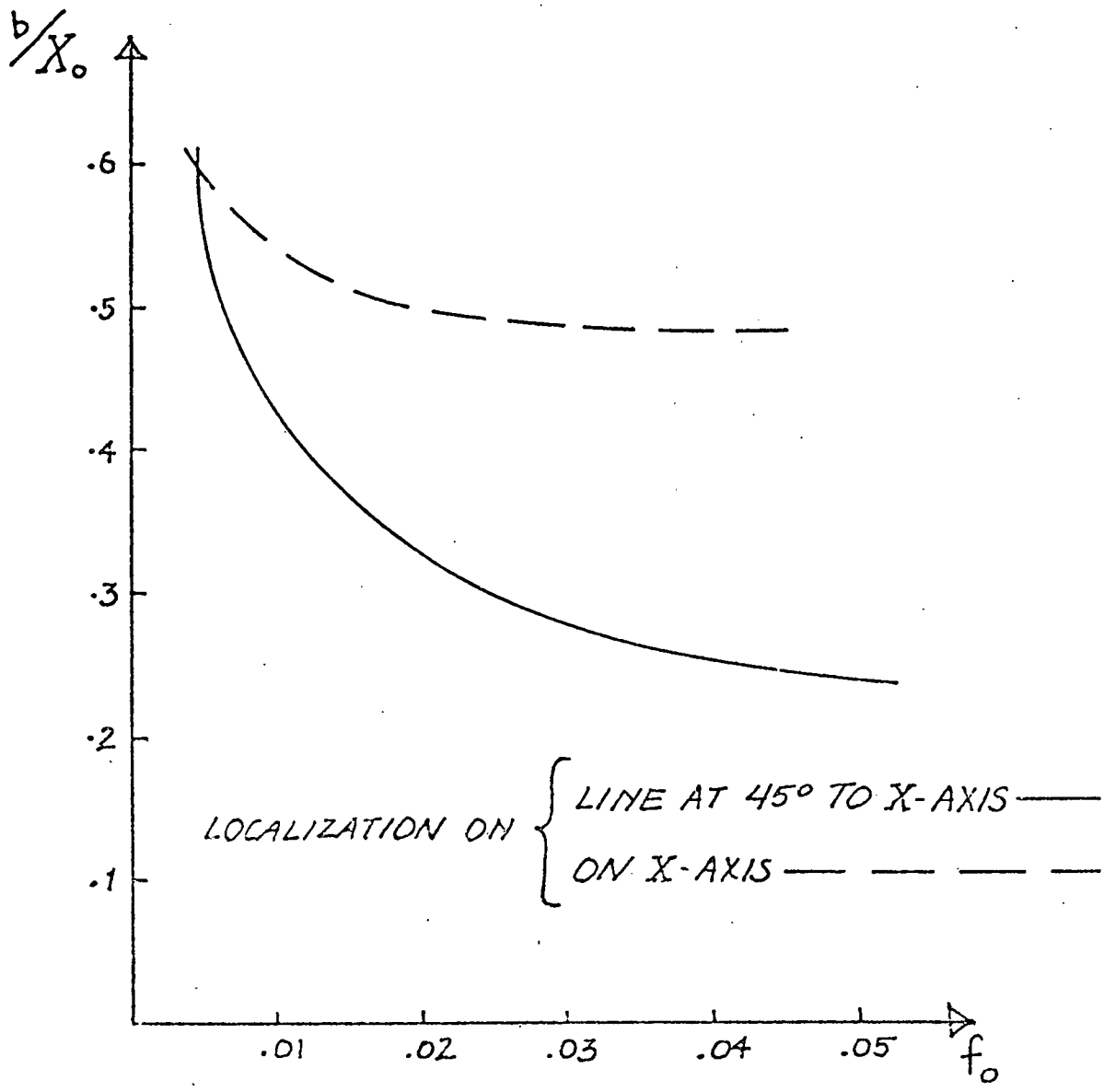
b/X₀
.6
.5
.4
.3
.2
.1
.01
.02
.03
.04
.05
f₀
LOCALIZATION ON
LINE AT 45° TO X-AXIS
ON X-AXIS